FACULTY OF SCIENCE AND TECHNOLOGY

# MASTER'S THESIS

| | |
|---|---|
| **Study programme / specialisation:**<br><br>**Mechanical, Structural and Materials Engineering** | **The *(~~spring~~/autumn)* semester,**<br>***(2023)***<br><br>**Open / ~~Confidential~~** |
| **Author: Darlington Ekene Ekemezie** | |
| **Supervisor at UiS: Prof. Raoof Gholami**<br><br>**Co-supervisors: Pål Østebø Andersen, Knut Erik Giljarhus, Mojtaba Ghaedi** | |
| **Thesis title: Hydrogen Diffusion through Caprock: On the Effect of Hydrocarbon Gas Composition** | |
| **Credits (ECTS): 30** | |
| **Keywords:**<br><br>**Depleted gas reservoir, Hydrogen storage, Caprock, Diffusion, Numerical simulation.** | **Pages:**<br><br>**+ appendix: 70 pages**<br><br>**Stavanger, *2023.*** |

## Abstract

Hydrogen storage in a depleted gas reservoir can be one of the most reliable options for seasonal, long-term, and large gigatons volume storage. Hydrogen loss due to molecular diffusion into caprock is one of the concerns of underground hydrogen storage in depleted gas reservoirs. This study evaluated the significance of hydrogen loss into caprock resulting from molecular diffusion. In particular, the impacts of pre-defused hydrocarbons inside the caprock were investigated.

For this purpose, one-dimensional models were created, and numerical simulation of hydrogen diffusion was performed using ECLIPSE 300. Moreover, chemical potential was used as the driving force for hydrogen diffusion and the model was assumed to have some previously diffused hydrocarbon components in the caprock. The fluid properties were modelled using the Peng-Robinson equation of state and the dissolution of gas in the water that occupies the pores of the caprock was neglected.

The results showed that the pre-defused hydrocarbons in the caprock influence the concentration and hence the cumulative loss of the hydrogen being diffused through the pores of the caprock. Other reservoir storage factors like pressure, temperate and porosity also play a vital role in this process. The hydrocarbons have been observed to limit the rate of diffusion into the caprock as the simulation goes from less dense to denser with respect to the pressure and temperature applied. Multiple gases of hydrocarbons also showed to limit cumulative loss to caprock at very low temperatures and high pressure. The gas composition at the boundary influences the caprock and reservoir interaction. Over time, the concentration value of hydrogen in the caprock in reservoir conditions indicates that hydrogen molecules will readily diffuse into the pores of the caprock.

The results also showed that hydrogen loss has a direct relationship with the porosity of the caprock, the gas saturation of the caprock, the square root of the diffusion coefficient, and the square root of time.

# Acknowledgements

This thesis is submitted in fulfilment of the requirements for the degree of master's in science at the University of Stavanger. I want to express my utmost gratitude to my supervisor Raoof Gholami and co-supervisors Pål Østebø Andersen, Knut Erik Giljarhus, and Mojtaba Ghaedi at the University of Stavanger for all their time and effort in helping me with this thesis. I would also like to extend my gratitude to the hydrogen research team at Equinor and especially to Alexandra Cely for her guidance in giving the field approach to numerical solutions. You all were always available whenever I had any questions about my research or writing and continually gave me the freedom to write this paper independently, while offering guidance when needed. I would also like to express my profound gratitude to my family and friends for providing me with continuous support and patience throughout my years of study and the process of writing this thesis.

Finally, I thank all my colleagues who gave me the necessary help to finish this degree and thesis successfully. This accomplishment would not have been possible without them.

Darlington Ekenedilichukwu Ekemezie

University of Stavanger

June 2023.

# Table of Contents

# List of Figures

# Nomenclature

$V_G^H$ = *total capacity for hydrogen in reservoir*

$V_R$ = *reservoir geometric volume*

$S_{wi}$ = *irreducible water saturation*

$P$ = *Pressure*

$V$ = *molar volume*

$T$ = *Temperature*

$P_o$ = *Standard Pressure*

$T_o$ = *Standard Temperature*

$T_C$ = *Effective critical temperature*

$P_C$ = *Effective critical Pressure*

$V_C$ = *Effective critical Volume*

$Z$ = *Gas compressibility*

$\sigma\theta$ = *Tangential stress*

$\rho$ = *Density*

$\Phi = porosity$

$g$ = *acceleration due to gravity*

$h$ = *reservoir depth*

$h_o$ = *the reference height*

$R$ = *Cavern radius*

$r$ = *radial distance of cavern*

$J_i$ = *molecular flux of component i per unit area*

$C$ = *total molecular concentration*

$V_m$ = *molar volume of mixture*

$D_i$ = *diffusion coefficient of component i*

$D_i^a$ = *activity- corrected diffusion coefficient of component i*

$D_i^T$ = *thermal diffusion coefficient of component i*

$\mu_i$ = *mole fraction of component i*

$\frac{\partial}{\partial d}$ = *gradient in the direction of flow*

$\frac{\partial P}{\partial h}$ = *pressure gradient*

$M_i$ = *molecular weight of the component i*

$\mu_{io} = reference\ chemical\ potential$

$fi = componenet\ fugacity$

$q = instantenous\ flux$

$Q$ = *rate of flow*

$K$=*permeability constant of the porous medium*

$A$=*cross-sectional area of medium*

$P_s$ = *Surface pressure*

$T_s$= *Surface temperature*

$P_g = pressure\ gradient$

$T_g = temperature\ gradient.$

$D_{ij}$ = *binary diffusion coefficient between component i and j*

$\rho_k^0$ = *zero pressure limit of molar density of phase k (k=oil, gas)*

$D_{ij}^0$ = *zero pressure limit of binary diffusion coefficient between component* i *and* j

$\rho_k$ = *molar density of phase* k

$\rho_{kr}$ = *reduced density of phase k*

$D_{ik}$ = *diffusion coefficient of component* i *in phase* k

$y_{ik}$ = *mole fraction of component i in phase k*

$C_1$ = *Methane*

$C_2$ = *Ethane*

$C_3$ = *Propane*

$C_4$ = *Butane*

$C_5$ = *Pentane*

$C_{i*}$ = *Concentration component 1m above the caprock*

$C_{i0}$ = *Concentration component 1m below the caprock*

$n_i$ = *number of moles of* $H_2$ *in the caprock i.e., the total loss of* $H_2$

$n_m$ = *number of moles in the reservoir*

$\frac{A_o}{A_{ocD}}$ = *function of diffusion coefficient skewedness, with a magnitude close to 1*

$C_{cap}$ = *concentration diffused into the caprock*

$C_{res}$ *concentration contained in the reservoir.*

$\overline{D}$ = *mean diffusion coefficient, a function of the activity corrected diffusion coefficient.*

# Abbreviations

IEA – The International Energy Agency

GHG – Green House Gas(es)

EOS – Equation of State

EOR – Enhance Oil Recovery

UGS – Underground Geological Storage

UHS – Underground Hydrogen Storage

GWh – Gigawatt-hour

TWh – Terawatt-hour

PVT – Pressure Volume Temperature

HC – Hydrocarbon

BWR – Benedict Webb Rubin

IMPES – Implicit Pressure, Explicit Saturation

AIM – Adaptive Implicit

*(Left Blank Intentionally)*

# Chapter 1: Introduction

## 1.1 Introduction

The International Energy Agency (IEA) projects that by 2030, the world's energy demand will increase by more than 70%, with fossil fuels continuing to account for 50% of this growth (Ball & Wietschel, 2009). At the same time, there is a need to control the emission of greenhouse gases (GHG) to avoid dangerous impacts on the climate system. Therefore, the challenge of finding the best way to reduce emissions while also providing the energy necessary for sustaining livelihood becomes essential. Hydrogen is a sustainable energy choice because it can be generated utilizing clean energy sources like solar or wind power. It is often referred to as green power gas because, when burned, hydrogen does not produce any harmful greenhouse gases or other pollutants, in contrast to conventional fossil fuels. As a critical future low-carbon energy carrier for decarbonizing transportation, power, heating, and so many different applications, hydrogen is garnering attention on a global scale. To this effect, efficient, dependable storage for hydrogen is needed to close the gap of green fuels in the energy mixing and hence give more utilization value to this gas.

The depleted natural gas reservoir has proven practical for storing natural gas for prolonged periods. The depleted gas reservoir is not with its challenges of caprock integrity, microbial activity, stress associated with P/T changes, and structural leakages, all associated with hydrogen storage (Kiran et al., 2023). Consequently, the underground storage of $H_2$ in geological formations like aquifers, depleted natural gas fields, or salt caverns is one way to deal with this issue. These locations offer a safe and economical way to keep substantial amounts of hydrogen in a condensed area. Additionally, the infrastructure required for natural gas extraction and storage can be adapted for hydrogen storage, making it a cost-effective option for large-scale storage.

This study will investigate diffusion mechanisms through caprock, a layer of impermeable rock that sits on top of a geologic formation where oil and gas are trapped. Caprock is a barrier preventing oil and gas from escaping to the surface. $H_2$ diffusion into the caprock occurs when molecules of $H_2$ gas migrate from the gas reservoir into the caprock because of the reservoir's

composition, chemical potential, pressure, and temperature gradients. We will analyse this concept while considering the effect of other hydrocarbon gases (ethane, methane) in the caprock and the effect of their thermodynamic properties on the diffusion rate.

## 1.2 Motivation of the Study

To cut down the cost of energy and make readily available green alternatives, a more sustainable and loss-proof process will need to be adopted. The bulk storage of $H_2$ in the depleted gas reservoir has checked all these solutions but still has its challenges, as mentioned earlier, with one of the most common caprock diffusion. This challenge has yet to be extensively studied, especially its causative mechanisms and ways to reduce and mitigate it in the long run. This work is born out of the need to investigate, numerically simulate and report the properties involved in the diffusion of $H_2$ into the caprock. Another motivation for this work is to predict the diffusive behaviour of the $H_2$ in the reservoir system in the presence of other reservoir hydrocarbon components, thus, to understand the properties of thermodynamics and the extent of influence in the diffusion of $H_2$.

## 1.3 Objectives

Given what was mentioned earlier in the introduction, this study aims to achieve the following objectives:

**i**. Build a numerical model to stimulate hydrogen storage in a depleted gas field.

**ii.** Simulate $H_2$ diffusion from the reservoir into the caprock based on the potential chemical gradient.

**iii**. Investigate the impact of different hydrocarbon components on the boundary concentration of $H_2$.

## 1.4 Thesis Structure

There are five chapters in this research. The context of this study is introduced in **Chapter 1**, along with an explanation of the necessity for further research on hydrogen diffusion through

caprock. The literature review is found on **Chapter 2** which includes an overview of hydrogen storage and environmental situations, storage limitations, diffusion mechanisms and potential thermodynamic interactions in depleted gas reservoirs in the presence of hydrogen and other hydrocarbon components. The technique is covered in **Chapter 3** and includes an overview of the many simulations used in this study, a description of the numerical simulation process, and methodology followed for each individual test. Additionally, **Chapter 4** includes the results, findings, and analysis of each individual test and the study's discussions. Conclusions, recommendations, and the necessary follow-up research are covered in the last section, **Chapter 5**.

# Chapter 2: Literature Study

This chapter contains generic literature about gas reservoir storage. It creates an understanding of the subject and help create a background study used to develop a model for the hydrogen diffusion problem and hence the thermodynamic effect by other hydrocarbon gas composition. This will make meaning to solving storage problems associated with hydrogen and other energy carrier gases and help in understanding the diffusion context.

## 2.1 Introduction to Underground Hydrogen Storage

The need to store billions of cubic meters in quantity of hydrogen in an already existing structure births the technology for underground storage. The ability of the caprock overlaying the underground reservoir to seal off the underground reservoir is a crucial factor in underground hydrogen storage in a depleted gas field or an aquifer. Porous caprock is frequently water-saturated, but when gas is applied up to the so-called "capillary threshold" pressure, it becomes hydraulically impermeable. It is often believed that because the gas build-up has been around for millions of years, the caprocks of depleted gas reservoirs will cling tightly to the gas. In the use of salt as caprock or surrounding rock in the caverns, tight rock salt is a widely impermeable barrier for liquids and gases (Reitenbach et al., 2015).

## 2.2 Energy Transition and the Need for Hydrogen

Green gases have proven to be key components to reaching the net zero goal. These green gases are sustainable and are derived from renewable resources including biomass, biogas, and hydrogen, and can take the place of fossil fuels in several processes like transportation, heating, and power generation. Biogas, for instance, is produced from organic waste and used to generate electricity or heat. It can also be upgraded to biomethane, which can be injected into

the natural gas grid or used as a transport fuel (Hebei Wansheng Environmental Protection Engineering Co., 2023). Hydrogen, on the other hand, can be produced from renewable electricity and used as a fuel in fuel cell vehicles or as a substitute for natural gas in industrial processes. Hydrogen is going through an extraordinary historical period for its crucial future significance in this global energy situation. This is because of its potential to be clean and renewable, efficient in combustion, high energy density by mass of 33.3kWh/kg, and a good research topic for academia. The major importance being that it is a carbon-free fuel, this means that there is no $CO_2$ emission when hydrogen undergoes combustion to produce either heat or electricity or both.

$$2H_{2_g} + O_{2_g} \xrightarrow{yields} 2H_2O_g + energy \quad (2.1)$$

In industries where it is difficult to minimize carbon emissions, hydrogen could replace conventional fossil fuels (e.g., cement farms, iron and steel production). Additionally, hydrogen provides a solution to the problem of seasonal storage related to renewable electricity generation, which peaks in the summer while consumption peaks in the winter. Despite these technical promises, hydrogen remains prohibitively expensive up to $16.80/kg and this is majorly influenced by the capital cost of production compared to other power generation (Capurso et al., 2022).

Green hydrogen derived from the electrolysis of water, using renewable energy sources such as wind, solar, or hydroelectric power has the potential to start a positive cycle for future renewable energy-based electricity grids since it can give power systems the much-needed flexibility and function as a backup for intermittent renewable energy sources. Excess energy from conventional and renewable power plants can be stored as hydrogen and used to generate electricity (using fuel cells or power systems), heat (using combustion), or both (co-generation), significantly reducing the output of greenhouse gases.

In conclusion, given the current great and widespread enthusiasm growing towards hydrogen, there is a need to focus on the effects that it can entail in different sectors in terms of renewable source exploitation, reduction of $CO_2$ emissions and the positive economy derived from commercializing its utilization. Each roadmap aimed at deploying hydrogen is constituted by three main milestones (production, storage, distribution, and final use). The role of hydrogen in the energy transition in the future energy scenario will need increased hydrogen-based

energy produced by renewable sources (green hydrogen) and it will play a key role in energy transition.

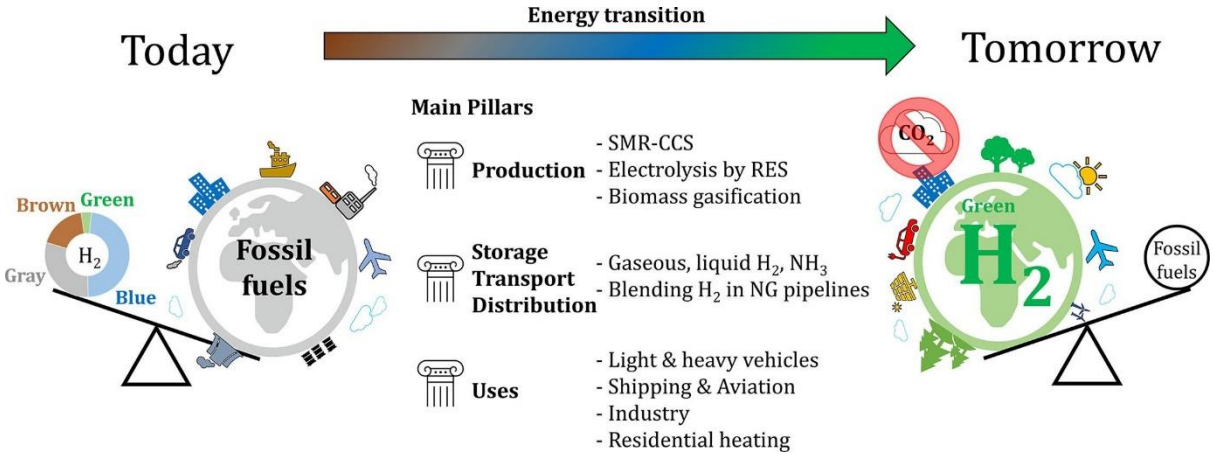


**FIG 2.1:** The role of green hydrogen in the roadmap for faster transition **(CAPURSO ET AL., 2022)**

## 2.3 Hydrogen Storage

As a vital potential low-carbon energy carrier essential for decarbonizing transportation, power, and heating as well as fuel-energy intensive businesses like the chemical and steel industries, hydrogen is garnering attention on a global scale. The fundamental problems of renewable energy generation, their intermittency, and their seasonal and geographical limitations, can be lessened with the use of large-scale hydrogen storage. Renewable energy sources are mostly dependent on seasonal variations in meteorological conditions (such as variations in sunshine levels and intensity or wind speed), which when paired with yearly variations in energy demand can lead to excesses or deficits in renewable energy (Heinemann et al., 2021). As a result, the entire system's energy requirement cannot be met by renewable energy alone. Extra renewable energy can be electrolyzed into hydrogen (sometimes known as "green hydrogen") and stored for usage when there is a strong demand for energy. Even hydrocarbon-derived hydrogen combined with carbon capture and storage, or "blue hydrogen," can assist in lowering emissions in the energy sector as we move toward low-carbon businesses (Heinemann et al., 2021).

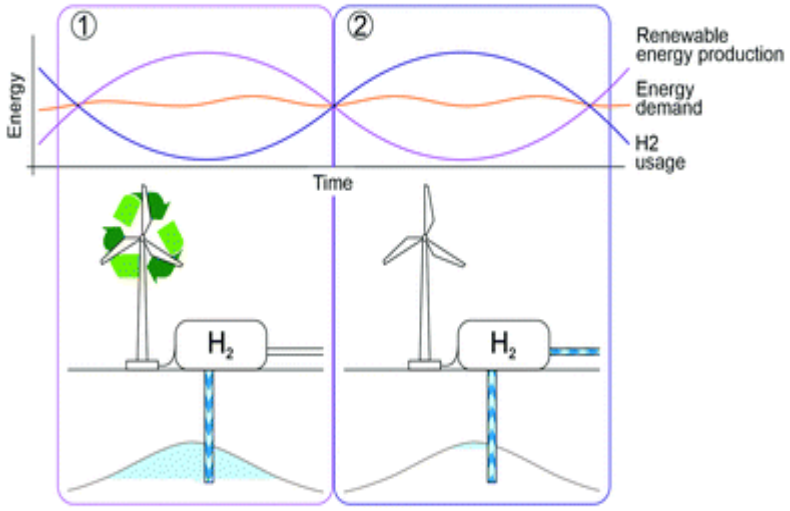


**FIG 2.2**: Hydrogen from renewable energy is stored during the high energy availability period(1) to satisfy demand during times of high energy demand and low renewable energy production (2) **(HEINEMANN ET AL., 2021)**.

The effective and loss-proof technology lies in the storage option adapted and needed to complement the production of this gas especially for storage over longer periods of time (months), the salt cavern with a capacity of storage in (GWh), porous saline aquifers and depleted hydrocarbon fields with capacity of storage in (TWh) all classified as Underground Geological Storage (UGS). The depleted hydrocarbon fields which offer large storage capacities to supply energy with over 1000TWh of energy value supplied especially during high peak demand periods around the world (Hassanpouryouzband et al., 2022).This is without neglecting the challenges posed by its physical properties and economics (site preparation, working gas capacity, cushion gas requirements, deliverability rates, cycling capability, maintenance costs, etc.), which determine its suitability for certain uses. This gas can also be stored on the surface which involves the technology of use of tanks or cylinders to store gas or liquid hydrogen. However, the amount of hydrogen that can be stored on the surface is constrained, and handling and storing hydrogen at high pressures or low temperatures poses safety issues. In Practical terms, the underground storage option has more acceptable and vast technological applications. Porous geological formations, such as depleted gas fields, which have a porous and permeable reservoir formation, a caprock, and a trap structure, offer the largest storage and discharge capacities. Injected hydrogen displaces the formation fluids with vertical migration prevented by the impermeable caprock and lateral migration prevented by the 3D trapping structure, allowing the stored gas to be injected, stored, and recovered

(Hassanpouryouzband et al., 2022). The concept of Underground Hydrogen Storage UHS is gaining attention, especially in research, but to ensure the suitability of the site for UHS, several factors such as gas storage capacity, caprock integrity, chemical stability, and microbiological interactions are critical.

### 2.3.1 Depleted Hydrocarbon Field

A geological trap that contains hydrocarbons and is covered by an impermeable layer known as caprock is recognized as a hydrocarbon reservoir. These reservoirs (oil or gas) are geological traps that have gone through several diagenetic stages where the physical and chemical changes occurring during the conversion of sedimentary rock (source rock, migration, and time) (Ghaedi et al., 2023). As a gas field nears the end of its useful life, it is frequently converted into a gas storage facility. Often, a depleted gas reservoir is characterized by low pressure and high-water saturation in the zone originally occupied by the gas. This is because aquifer water displacement has caused the gas to be displaced from the reservoir. Depleted gas fields have also shown their resistance (imperviousness) throughout geological time and so can be employed to store gases. These geological structures might be permeable for storage opportunities and are often combined with low-permeable and non-fractured sealing rocks (Kiran et al., 2023). These structures may appear to be practical for storing gas but requires in-situ conditions like pressure, temperature and geomechanical rock stresses because the properties for UHS are significantly different from regular oil and gas. The depleted gas and oil reservoirs are available in abundance and can pass for an already existing geological structure (Kiran et al., 2023). Depleted gas reservoirs can provide gigaton capacity and the necessary infrastructure for large-scale hydrogen storage (Muhammed et al., 2023). Hydrogen in a depleted gas reservoir offers the potential for the seasonal storage of essential energy and hydrogen production from electrolysis of water during periods of excess energy availability (Amid et al., 2016). However, a significant issue with these storage locations is the high molecular diffusion of hydrogen.

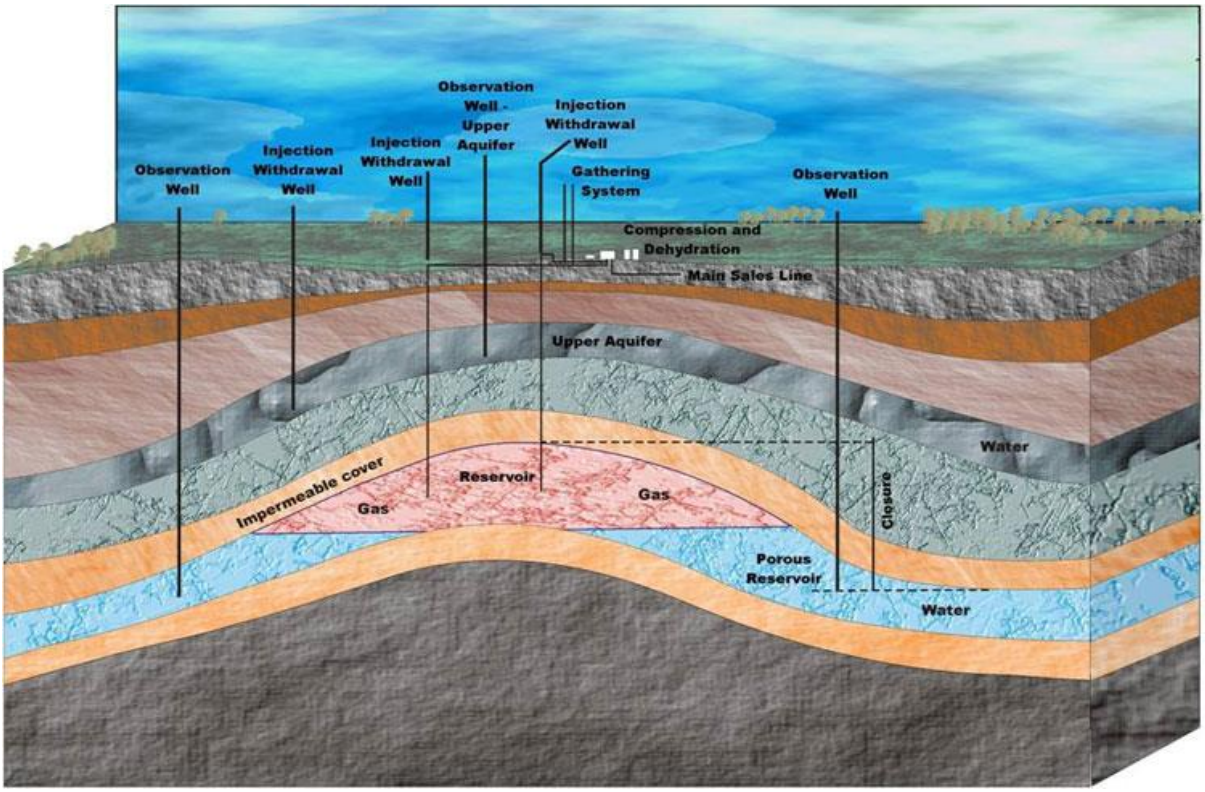


**FIG 2.3:** Schematic representation of an underground hydrocarbon reservoir structure capable of Hydrogen storage **(STOREY, 2013)**.

For a depleted gas reservoir with depth below the seabed, 2743 m; Temperature, $T = 365$ K; Initial pressure, 31.3 MPa, as indication of the maximum pressure that the reservoir could withstand; main material was sandstone of porosity $\varphi = 0.2$ and permeability to methane 75 mD (or $7.4 \cdot 10^{-14}$ m$^2$). The amount of hydrogen that could be stored in a reservoir; sandstone reservoirs with a varying proportion of carbonates present as cements (from less than 1% to up to 24%) (Amid et al., 2016) can be derived from the Eq. ( 2.2) given below at standard conditions:

$$\frac{V\frac{H}{G}}{V_R} = \frac{Y_H \ \ \varphi(1 - S_{wi})P}{ZP_\circ}\frac{T_\circ}{T} \qquad (2.2)$$

Where $V_G^H$ is the total capacity for hydrogen, $V_R$ is the rock bulk volume (i.e., the reservoir geometric volume), $Y_H$ the volume fraction of hydrogen in the gas, $S_{wi}$ the irreducible water saturation (i.e., the fraction of water that remains in the pore volume when gas is stored), estimated at $\varphi = 0.2$ in this reservoir. $P$ and $T$ are the reservoir temperature and pressure,

respectively, $Z$ the compressibility, and $P_o$ and $T_o$ are the temperature and pressure at standard conditions (0.1Mpa/ 1atm and 273 K, respectively).

The depleted gas reservoir is significant to this study because of its challenges as mentioned earlier in the hydrogen storage introduction, with the challenge of caprock integrity being the centre of focus for this study.

### 2.3.2 Saline Aquifers

The saline aquifer is one of the Underground Storage (UGS) options for hydrogen gas presently explored. This presents a vast potential for prolonged periods of cost-effective storage without significant loss, this is because rock formations and the salty water function as a natural barrier to stop leaks or contamination of hydrogen that has been stored. Saline aquifers are also suitable for large hydrogen storage because they are typically located deep underground and often under high pressure (Jafari Raad et al., 2022). An aquifer storage operation does not involve brine disposal or freshwater injection; hence the chance of contaminated hydrogen being stored is quite minimal. This provides a unique opportunity for the renewable energy industries to contribute to the worldwide clean energy transition.

Saline aquifer hydrogen storage is like $CO_2$ sequestration and natural gas storage from a technological and practical standpoint. A typical aquifer storage system consists of wells for injecting into and withdrawing from the target formation layer, pipelines linking the wells to the surface facilities, and a confining brine-saturated formation layer holding the injected gas (i.e., gas-processing, and electrical equipment). The injected hydrogen is divided into a cushion gas and a working gas. Other gases can as well serve as cushion gas and that is the unrecoverable part of the injected gas, and its role is to maintain the reservoir pressure at an adequate level providing the designed deliverability (Jafari Raad et al., 2022). Working gas is part of the injected gas that is repeatedly charged and discharged during the cyclic injection/reproduction periods. Compressed hydrogen is injected into a target formation's perforation interval in a hydrogen storage setup. The thickness of the geological formation may vary from 10 to 100 m (Jafari Raad et al., 2022). The hydrogen is pushed into the originally brine-saturated formation pore spaces by the injection-induced pressure in the wellbore and the vicinity of the perforation zone, replacing the pre-existing brine.(Ball & Wietschel, 2009).

Saline aquifers present a huge opportunity for economical and sustainable large-scale hydrogen storage. Saline aquifers are frequently the only accessible geological formations within a reasonable driving distance of sources of renewable energy, creating a rare opportunity for the renewable energy industry to aid in the global transition to cleaner energy. However, there has never been a case of pure hydrogen being stored in saltwater aquifers.

### 2.3.3 Salt Caverns

The salt caverns are designed to store hydrogen with the consideration of a good geological salt formation. Caverns sited within a good salt deposit are of importance for the successful solution mining leaching (circulation) and construction process. Direct and indirect (reverse) leaching are the two primary leaching techniques utilized in solution mining technology. In the direct leaching method, freshwater is pumped into the cavern, it sinks through an inner leaching string to the bottom of the wellhole (Heinemann et al., 2021). Freshwater runs outside the leaching string to the cavern roof, gradually saturating it. The inner and outer leaching strings allow the brine to exit the cavern. By using the indirect or reverse leaching method, freshwater enters the cavern through the outer and inner string, mixes with the brine, and then rises to the roof. Leaching on the cavern's roof is restricted by a protective covering, and these blanket does not dissolve in salt, and it is a material lighter than freshwater or unsaturated brine.

Both approaches yield different shapes of the cavern as direct leaching gives a cylindrical shaped formation while the reverse leaching gives an enlarged top formation and can be combined in the leaching process or used differently depending on the geological suitability of the salt formation (Katarzyna, 2020).

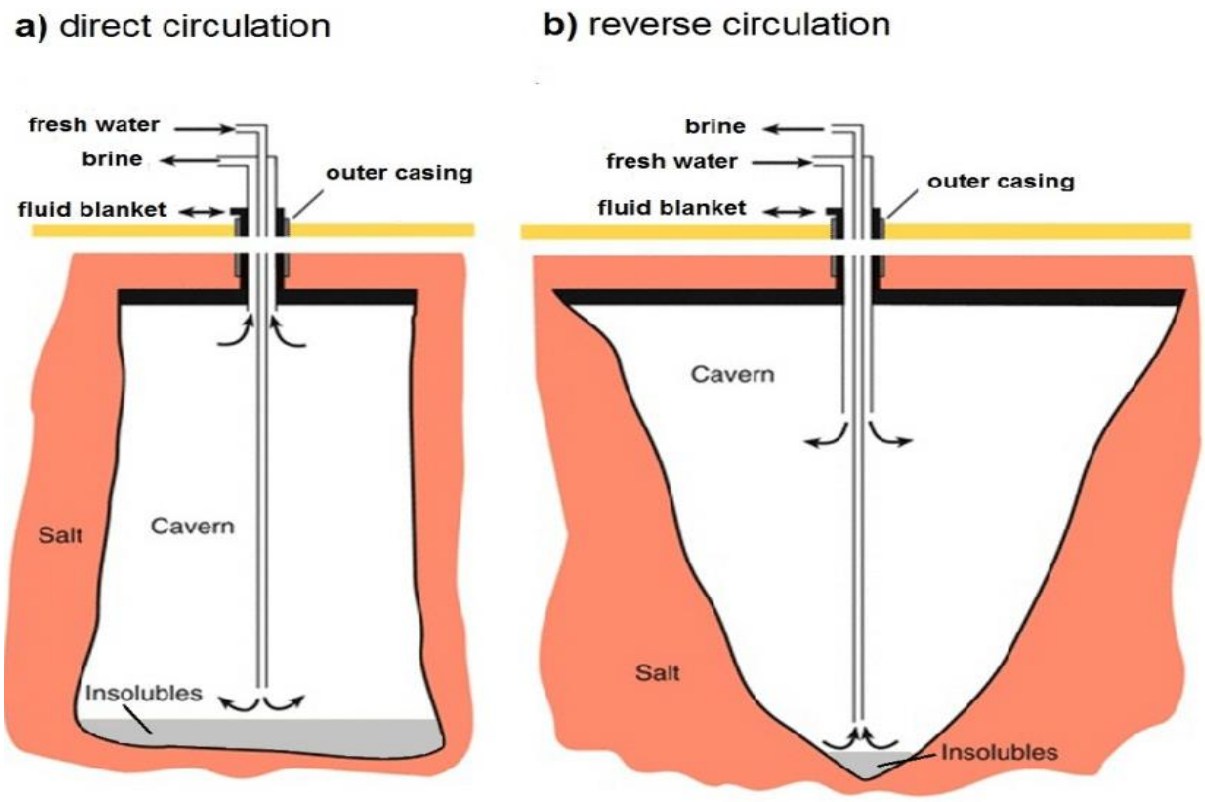


**FIG 2.4**: Schematics showing the direct and indirect leaching process **(KATARZYNA, 2020)**

For efficient storage, hydrogen gas is compressed in underground salt caverns up to a pressure of 20 MPa and above(Ozarslan, 2012). Below is a schematic representation of hydrogen production and compressed gas storage facility in a salt cavern. The primary parts include compressors for gas injection and withdrawal, wind turbines and solar PV modules to produce renewable electricity, electrolysers to create hydrogen and oxygen from water, and a gas combustion power plant to do so using hydrogen as fuel.

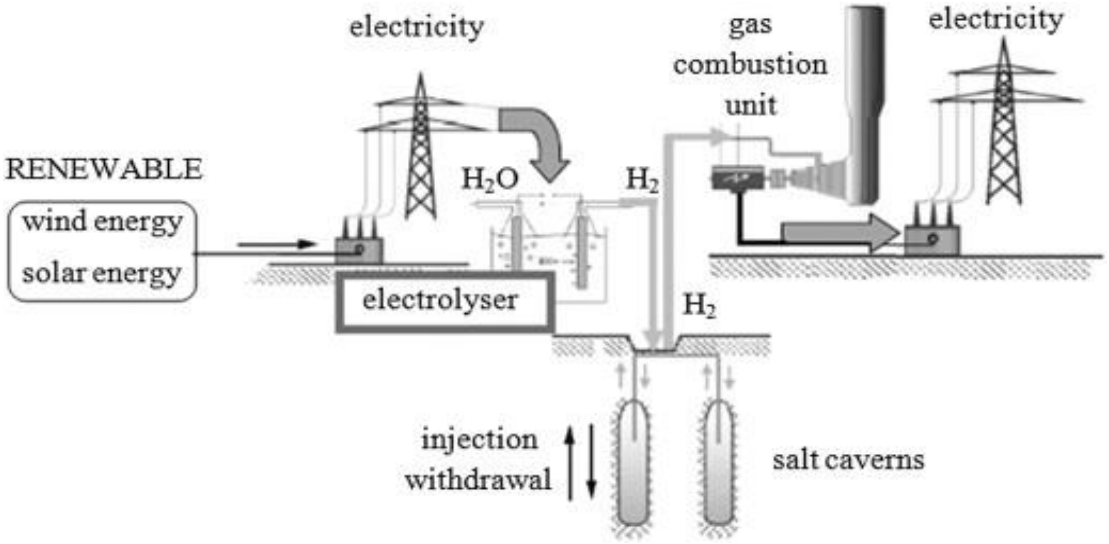


**FIG 2.5**: Schematic view of a salt cavern facility for hydrogen production and gas storage **(OZARSLAN, 2012)**

The storage option of the salt cavern is tipped on geological impermeable rocks which has the a unique advantage in that it does not react with hydrogen and the rock salt is very gastight (Ozarslan, 2012). This technology has its limitations which may arise from dilatancy i.e., when granular materials (salt) are subjected to shear stress, the grains reorient themselves, allowing them to rearrange and create void spaces between them. This may in turn increase rock salt permeability and decrease in strength. As a result, salt caverns for storage need to be carefully built-in accordance with the salt quality of each site and the operational requirements.

Prior to the development of the storage structure, the rock medium for an underground rock structure like a cavern is initially stressed. The vertical starting stress component ($\sigma\theta$) for deep salt deposits can be calculated, the formula assumes isotropic conditions, meaning that the mechanical properties of the salt are assumed to be the same in all directions. It provides an estimation of the stress distribution based on the weight of the overlying rock column. The stress distribution within salt caverns can be estimated using the following simplified formula, known as the cylindrical solution for isotropic conditions:

$$\sigma\theta = \left(\frac{\rho g h}{2}\right)\left(1 - \left(\frac{R^2}{r^2}\right)\right) \qquad (2.3)$$

where σθ is the tangential stress (in the circumferential direction), ρ is the density of the salt, g is the acceleration due to gravity, h is the depth below the ground surface, R is the radius of the cavern, r is the radial distance from the centre of the cavern.

It is also crucial to keep in mind that the equation assumes a simplified scenario and does not take into consideration the complexity of many soil or rock layers, groundwater conditions, or other elements that can affect how stresses are distributed in the subsurface. Operating gas pressure restrictions for salt caverns are typically determined by site-specific geomechanical evaluations, conventional criteria, and already-in-place laws.

## 2.4 Hydrogen Loss in Geological Storage Sites

According to the review, the main factors that cause hydrogen losses in the subsurface are hydrodynamics, geochemistry, and microbiological processes (Kiran et al., 2023). Gas storage in depleted reservoirs is impacted by the injection strategy, reservoir characteristics, quality, and operational parameters (Tarkowski, 2019). Hydrogen having greater diffusivity than methane is required to estimate the scale of its loss through the underlying aquifer and the cap rock above (Amid et al., 2016). The diffusivity coefficient of hydrogen is very high, and the fracture sizes will have a significant impact on storage and integrity (Kiran et al., 2023).

There are several uncertainties that can be considered in hydrogen loss, but because caprock integrity is less studied and hence not much of a body of knowledge has been developed from it, these encourage the motivation for this work and the need to investigate this uncertainty. Specifically, caprock failures depend on porosity, permeability, interfacial tension, and capillary pressure, which promote the stored gas's leakage. Capillary sealing efficiency is frequently used to determine the integrity of caprock in storage sites. This effectiveness is influenced by fluid densities, wettability, interfacial tension, and caprock threshold pore sizes. The effects of caprock mineralogy, mineral content, salinity, temperature, pressure, and salinity on the capillary sealing effectiveness should also be considered.

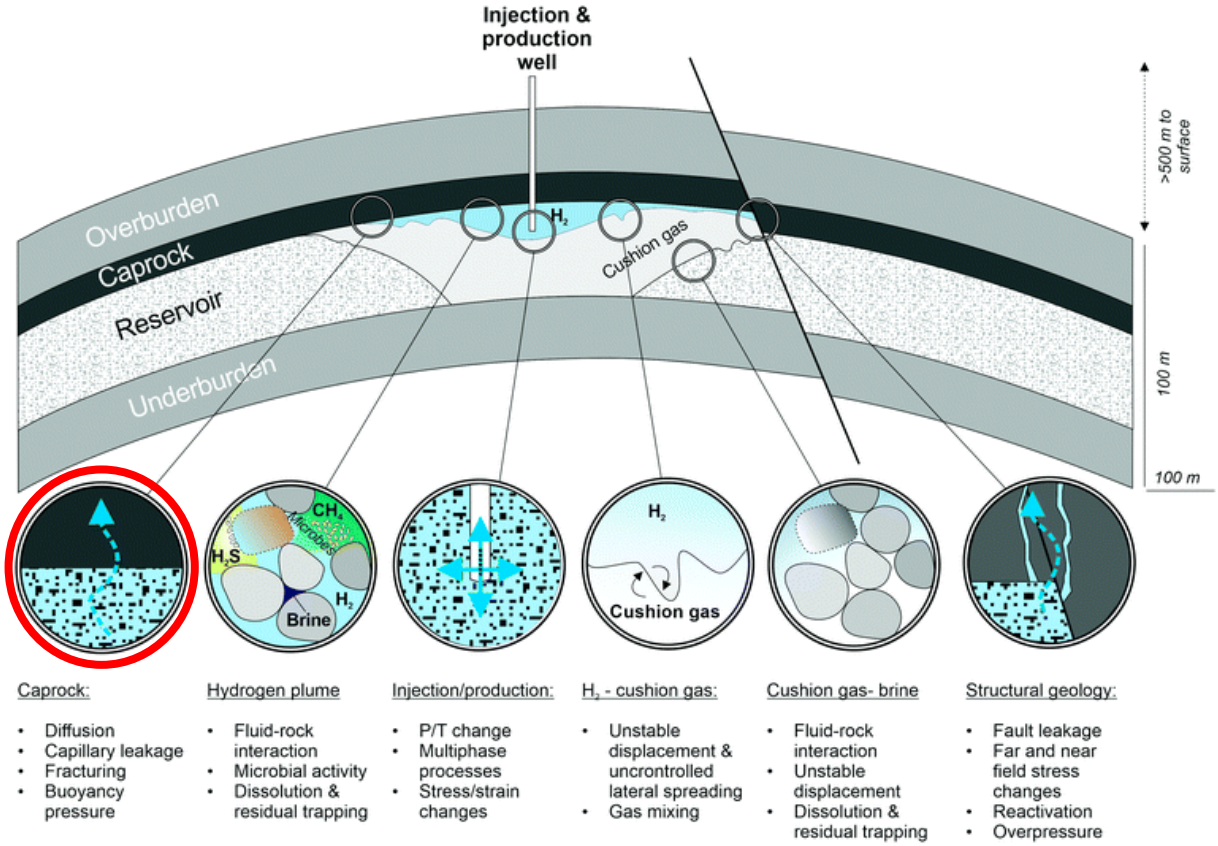


**FIG 2.6**: Hydrogen storage in porous media highlighting all geological uncertainties (HEINEMANN ET AL., 2021).

## 2.5. Hydrogen Diffusion

$H_2$ diffusion is the process by which molecules of the gas are moved from one area of a system to another due to an increase in chemical potential which creates a gradient that drives diffusion. This gradient may result from variations in concentration, temperature, pressure, or other factors. Likewise, the concept of hydrogen diffusion through the caprock involves the molecular migration of this gas charged by the concentration gradient in the reservoir-caprock system, chemical potentials of the hydrogen gas or some thermodynamic inhibitory properties like temperature and pressure causing an effect in the system.

Molecular diffusion is commonly described using Fick's Law, a model referred to as Fickian diffusion. Fickian law is based on no mixture and independent transfer of molecules without interaction with the molecules of other mixtures. For low permeability and low-pressure systems, where the pore sizes are of the same scale as the mean free path of the gas molecules,

an enhancement to diffusion occurs by a process known as Knudsen diffusion. The diffusion caused by the concentration gradient is given as:

$$J_{i} = -CD_{i}\frac{\partial x}{\partial d} \quad (2.4)$$

Noting that gas concentration driven diffusion is non-ideal for gas and liquid at high pressure.

The chemical potential gradient emerges as the suitable driving force for each component's diffusion, giving the behaviour a complex composition dependence in addition to that from pressure and temperature factoring the chemical, gravity, and thermal forces in the total potential of the diffusion flux, we have in Eq. ( 2.5).

$$J_i = -CD_i^{a}X_i\frac{1}{RT}\frac{\partial}{\partial d}[\mu_i - M_{ig}(h-h_o) + M_i D_i^T \ln T] \quad (2.5)$$

Where:

$J_i$: molecular flux of component *i* per unit area

C: total molecular concentration given by C = $\frac{1}{V_m}$

$V_m$: molar volume of mixture

$D_i$: the diffusion coefficient of component *i*

$D_i^a$ : activity- corrected diffusion coefficient of component *i*

$D_i^T$: thermal diffusion coefficient of component *i*

$\mu_i$ : the mole fraction of component *i*

$\frac{\partial}{\partial d}$ : the gradient in the direction of flow

$M_i$: the molecular weight of the component *i*

g: acceleration due to gravity

h: the height

$h_o$: the reference height.

T: the temperature

R: the chemical potential of component *i*, given by a constant $\mu_i$

$$\mu_i = \mu_{io} + RT \ln(fi) \qquad (2.6)$$

where $\mu_{io}$ reference chemical potential

$fi$ the componenet fugacity

This molecular migration is highly influenced by the entropic motion of molecules of hydrogen in the reservoir system.

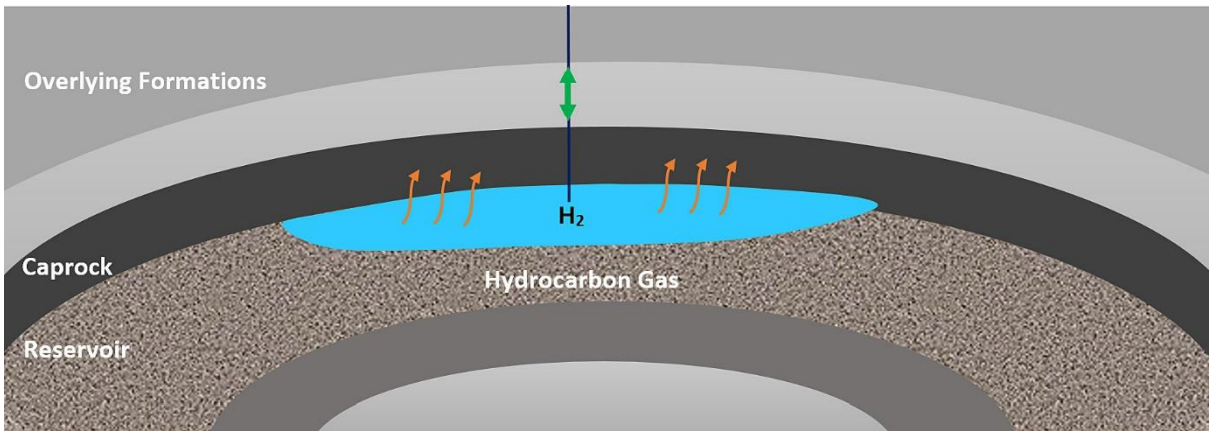


**FIG 2.7:**Schematic representation of $H_2$ storage and diffusion through caprock **(GHAEDI ET AL., 2023)**

## 2.5.1 Diffusion through a Porous medium

To perfectly understand the diffusion into porous surface medium in this case caprock, the application of Darcy's law in an equation that describes the gas flow through the medium will come in handy. The law which states that the flux is proportional to the pressure gradient has its limitations because the variation of permeability is unknown, solving the equations governing the diffusion when the permeability of the matrix changes during the process provides significant analytical challenges, a technical reason why the study and application of diffusion is devoted to diffusion flus rather than pressure. The equation is shown as:

$$Q = -KA\left(\frac{\partial P}{\partial h}\right) \qquad (2.7)$$

where: $q = \frac{Q}{A} is\ the\ instantenous\ flux,$ Q is the rate of flow $m^3/s$, K=permeability constant of the porous medium, A=cross-sectional area of medium $m^2$, $\frac{\partial P}{\partial h}$ = pressure gradient.

However, Darcy's law allows the flux to be obtained directly from pressure gradient (Caputo & Plastino, 2004). While the flow can be assumed to be a Stokes flow at exceptionally low flow velocities, this law approximates the Navier-Stokes equation. A continuum assumption underlies the fundamental Navier-Stokes equation for gas flows, which is only true if the mean free path of the molecules is significantly shorter than the system length scale (Basu & Singh, 1994). In a porous medium, the fluid flow rate is calculated using Darcy's equation, whereas the fluid density change rate is determined using the continuity equation. The merging of the two equations and its deductions can help in predicting the fluid (gas) flow through a porous media over time (Basu & Singh, 1994).

## 2.6 Reservoir Pressure-Volume-Temperature

Pressure-Volume-Temperature (PVT) is an important analysis of reservoir gas technology. It gives key information about the behaviour of fluids in a reservoir. This data is utilized to understand hydrocarbon properties such as density, viscosity, compressibility, and phase behaviour of reservoir fluids, which are crucial in assessing recoverable reserves and optimizing hydrocarbon production. P-V-T analyses are used in reservoir gas technology to determine the behaviour of gas under varied pressure and temperature circumstances. This data is then utilized to develop reservoir models and estimate the performance of gas reservoirs, which can be used to optimize hydrocarbon production and recovery. The P-V-T measurement is also essential for determining the reservoir's hydrocarbon composition. The gas composition affects the fluid's physical and chemical properties and determines the kind of processing required for efficient production. These measures serve as basis for calculations of the reservoir's oil content, production capacity, and variations in the ratios of generated gas to oil over the reservoir's production life. This can also be applied to hydrogen storage. Hence calculating its reservoir recovery efficiency also requires P-V-T relations (Oistein, 1980).

### 2.6.1 Pressure and Temperature of a Reservoir System

The major dominant changing conditions that affect the overall performance of the reservoir system are pressure and temperature. As they vary throughout the system, so does the volume and fluid behaviour of the contained fluid also vary. Pressure and temperature gradients, which are at the basis of most issues involving the transport of oil and gas through the rocks, are determined by differences in fluid pressure and temperature between one location and another. Defining reservoir pressure and temperature with respect to depth will play a critical role in determining the thermodynamic flow properties of the fluids present and the fluid properties of the reservoir. Several types of reservoirs can be defined by the location of the initial temperature and pressure and Fig 2.8 gives a P-T phase diagram for a reservoir fluid. The region covered by the bubble-point and dew-point curves depicts combinations of pressure and temperature where both liquid and gas phases can occur. The percentage of total hydrocarbon volume that is liquid for any temperature and pressure is displayed on curves within the two-phase envelope (Oistein, 1980). The hydrocarbon combination will be liquid at pressure and temperature values that are above the bubble-point curve. The hydrocarbon mixture will be in a gas phase at pressure and temperature points that are above or to the right of the dew-point curve. The critical point indicates a mathematical discontinuity, and phase behaviour close to this point is challenging to define. The critical point is where the bubble-point, dewpoint, and constant quality curves converge (B.C Craft, 2014). Considering hydrogen storage in a depleted gas reservoir in a compressed gas state, temperature ranging above 300°F (149 °C) and quite above 3900psi (269 bar), since this phase lies outside the liquid-gas two phase region and to the critical point, the fluid is said to be in a one-phase gas state. As the hydrogen remains at temperature, it is evident that it will remain at that gas phase as pressure declines.

The field approach to defining the P-T of a reservoir, surface pressure, temperature, pressure, and temperature gradient with respect to depth of reservoir type being considered is highly considered. The mathematical equations applied to help derive the P-T values are:

$$\mathrm{P} = P_s + P_g \times reservoir\ depth \qquad (2.8)$$

$$T = T_s + T_g \times reservoir\ depth \qquad (2.9)$$

where: $P_s$ = Surface pressure in bar, $T_s$ = Surface temperature ℃, $P_g$ = pressure gradient $0.1\text{bar/m}$, $T_g$ = temperature gradient $0.03℃/\text{m}$ , reservoir depth in m (All in metric unit of measurement).

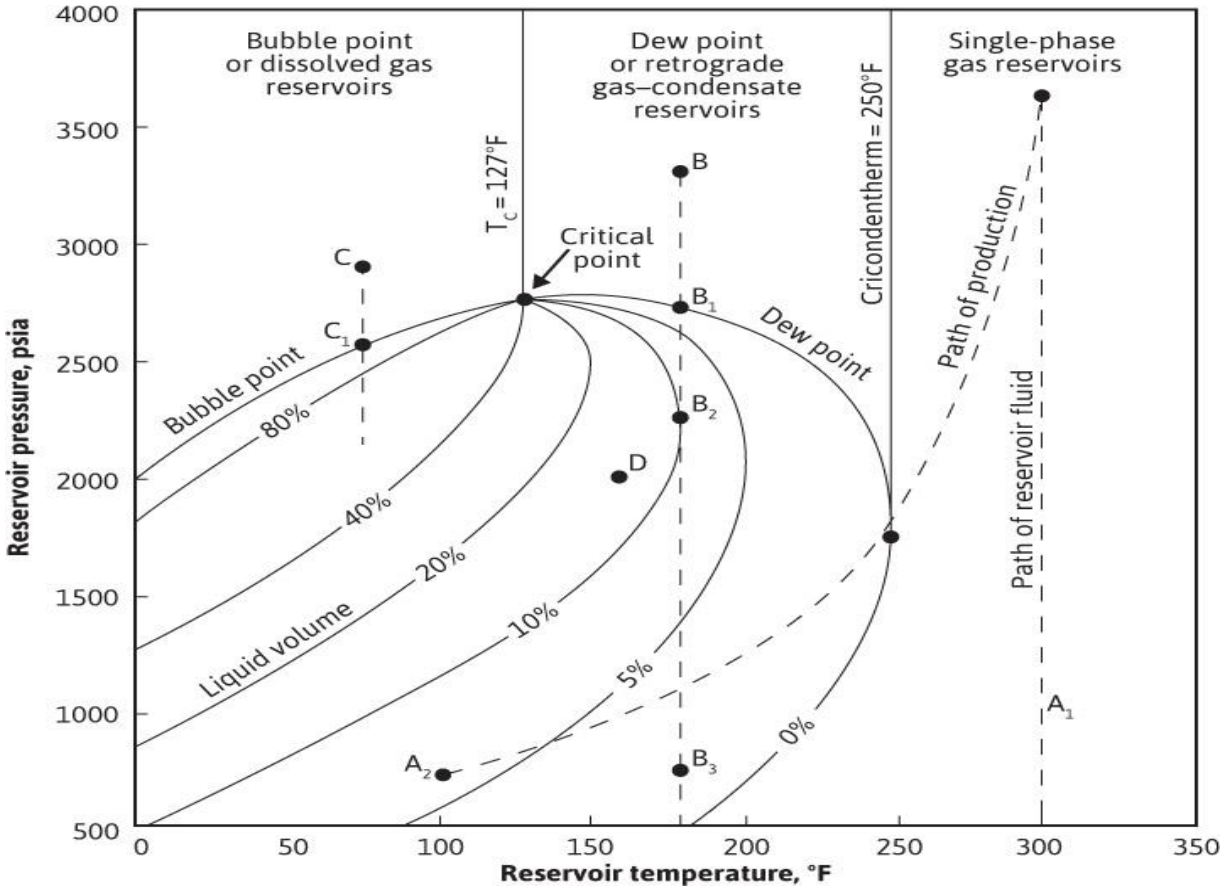


**FIG 2.8**: Pressure-temperature phase diagram of a reservoir fluid **(B.C CRAFT, 2014)**.

## 2.6.2 P-T relationships and diffusion coefficient

Diffusion is a key factor in procedures like gas injection in fractured or heterogeneous reservoirs and gas diffusion through cap rock. Although these processes take place in porous oil and water-saturated rock, formation resistivity data can be used to simulate the effect of the rock's tortuosity on diffusion data pertaining to bulk liquids (Matthews et al., 1987). The diffusion coefficients' relationships with pressure, temperature, and composition are helpful (i.e., the activity corrected diffusion coefficient). Also, there are many correlations, but when they are used to estimate reservoir conditions, their estimations might vary by wide range of

percent. In reservoir models of fractured reservoirs, the Sigmund correlation has been applied with some effectiveness utilizing an extension to the high pressures present in reservoirs at extreme depths (Helbæk et al., 1996).

**The Sigmund Correlation** is based off an experimental measurement of diffusion coefficients in the reservoir fluid. The correlation was proposed to predict and compare the binary diffusion coefficients for high pressure mixtures in the gas-liquid phase (Sigmund et al.,1976). His prediction is extensively used correlation for diffusion coefficient calculations. He developed his values from reported experimental data on measurements for hydrocarbon and petroleum systems at high pressure. The binary diffusion coefficient, between components i and j, is determined using Sigmund correlation as follows (Du & Nojabaei, 2020):

$$D_{ij} = \frac{\rho_k^0 D_{ij}^0}{\rho_k}(0.99589 + 0.096016\rho_{kr} - 0.22035\rho_{kr}^2 + 0.032874\rho_{kr}^3) \quad (2.10)$$

(Belery and da Silva, 1989) claimed that Eq.**( 2.10)** gave a negative $D_{ij}$at $\rho_{kr} > 3.7$ and then suggested the expression.

$$D_{ij} = \frac{\rho_k^0 D_{ij}^0}{\rho_k}(0.096016 \exp(3 - \rho_{kr})) \quad (2.11)$$

$\rho_k^0 D_{ij}^0$ is the zero-pressure limit of the density-diffusion coefficient product in phase k and calculated by:

$$\rho_k^0 D_{ij}^0 = \frac{0.0018583 T^{0.5}}{\sigma_{ij}^2 \Omega_{ij} R}\left(\frac{1}{M_i} + \frac{1}{M_j}\right)^{\wedge 0.5} \quad (2.12)$$

where: $D_{ij}$ binary diffusion coefficient between component i and j [$m^2/s$]

$\rho_k^0$ zero pressure limit of molar density of phase k (k=oil, gas) [$mol/m^3$]

$D_{ij}^0$ zero pressure limit of binary diffusion coefficient between component *i* and *j* [$m^2/s$]

$\rho_k$ molar density of phase *k* (*k* = oil, gas) [$mol/m^3$]

$\rho_{kr}$ reduced density of phase k

Sigmund went further to define the diffusion coefficient of component *i* in phase k of a multicomponent mixture based on Wilke formula (Wilke, 1950), as given in

$$D_{ik} = \frac{1 - y_{ik}}{\sum i \neq j \frac{y_{jk}}{D_{ij}}} \quad (2.13)$$

where: $D_{ik}$ diffusion coefficient of component *i* in phase *k* [$m^2/s$]

$y_{ik}$ mole fraction of component i in phase k

To estimate the diffusion coefficients in mixtures of multicomponent gases, Fuller, Schettler, and Giddings (FSG) model is an empirical correlation often used which is based off the Wilke diffusion theory. The relation between the diffusion coefficients and the molecular characteristics of the gas components, such as molecular weight and diameter, is considered. When calculating the diffusion coefficients for multiple gas (binary gas) mixtures using the FSG model, the Wilke diffusion coefficient is frequently included.

The Sigmund experimental base inspired the work done by (Mohammed et al., 1994), he proposed a straightforward procedure for utilizing a PVT cell to calculate the diffusion coefficients of dense gases in liquids. Thermodynamic equilibrium determines the end condition when a non-equilibrium gas is in contact with a liquid in a sealed container at a constant temperature. The diffusion process in each phase, however, helps to estimate the amount of time needed to achieve the ultimate state. At the gas-liquid interface, the two phases are always in thermodynamic equilibrium, although the position and pressure of the contact may change over time. The rate of diffusion in each phase and, consequently, the diffusion coefficients determine the rate of change of pressure and the position of the interface as a function of time. This method of evaluating diffusion coefficients does not need compositional measurements; as a result, it is less expensive than traditional techniques. Diffusion coefficients were found using this method to be within 5% of the values reported in the literature for the binary system of methane and n-pentane at 311 K and 70 bar. For the measurement of effective diffusion coefficients in reservoir fluids, the experimental technique can be easily adaptable to multicomponent systems (Riazi, 1996).

**The Stefan-Maxwells Relations**, which explain diffusion in low density gas mixtures, connect a component's mole fraction gradient to the mutual diffusion coefficient $D_{ik}$, composition, and differential in diffusion velocity $v$ between the component (in this case, $H_2$) and each of the mixture's other species (various HC gases) (Sigmund, 1976). Stefan described the process of diffusion, in which the (n-1) independent driving forces present in a mixture of n species determine the diffusive fluxes, Ji, of species over a plane across which no net movement of

moles happens. His prediction is that a species is not required to spread in the direction of its own force of motion. Consider binary species A and B, subject to the Fickian law and diffusion. The diffusive flux is given by:

$$J_i = C_A(V_A - V^*) = -CD_{AB}\nabla X_A \quad (2.14)$$

After some mathematical deductions, for Stefan-Maxwells formulation for ideal gas mixtures consisting of N number of species can be written as:

$$\nabla x_i = \sum_{j=i}^{N} \frac{x_i x_j (v_j - v_i)}{D_{ij}} \quad (2.15)$$

$D_{ij}$ is the binary diffusion coefficient

When we have N=2, the equation gives.

$$\nabla x_i = \frac{x_1 x_1 (v_1 - v_1)}{D_{11}} + \frac{x_1 x_2 (v_2 - v_1)}{D_{12}} = \frac{x_1 x_2 (v_2 - v_1)}{D_{12}} \quad (2.16)$$

The relevance of this model is that it can be used to analyse the transport of different gases in a mixture. By considering the concentration gradients and diffusion coefficients of the individual gases, one can determine the rates at which they diffuse and mix with each other.

**The Benedict-Webb-Rubin (B-W-R) equation** of state is a modification of the Van der Waals equation of state and considers the non-ideal behaviour of real gases. This includes parameters that describe the size and shape of the molecules in the gas, as well as their intermolecular forces. PVT properties of hydrogen and mixtures containing hydrogen can be effectively analysed by using the (B-W-R) equation, which has eight constants. These constants are obtained by substituting the experimental data in the B-W-R equation. The equation is given as:

$$\mathrm{P} = \mathrm{RTd} + \left(\mathrm{BoRT} - \mathrm{Ao} - \frac{Co}{T^2}\right) d^2 + (bRT - a)d^3 + a\alpha d^6 + \left(\frac{cd^3}{T^2}\right)(1 + \gamma d^2)^{-\gamma d^2} \quad (2.17)$$

where the constants of the B-W-R equation for hydrogen are given as:

$A_0 = 585.127$

$B_0 = 3.339 \times 10^{-4}$

$C_0 = 482.82 \times 10^4$

α = -98.597

ɓ = 868.2 x $10^{-4}$

c = 1423.17 x$10^{3}$

αα = 49.239

γ = 900.00 x$10^{-3}$

These constants can be used in the equation when T is in degree Rankine, d in lb. moles per cu.ft., P in p.s.i., and R=10.7335lb. cu. Ft. per (sq.in.) (lb. mole) (°R.).

The BWR (BENEDICT WEBB RUBIN) equation of state for hydrogen can also be simplified using the Peng-Robinsons equation of state in a more conventional unit as:

$$P = \frac{RT}{(V-b)} - \frac{a}{(V(V+b)+b(V-b))} \qquad (2.18)$$

where: P is the pressure at 70MPa.

V is the molar volume,

R is the gas constant,

T is the temperature at 298K

a and b as 0.2444 $Nm^4/mol^2$ and 2.74 x$10^{-5}$ $m^3$/mol respectively for hydrogen

The ideal gas law, which is represented by the first component on the right-hand side of the equation, assumes that the gas molecules are not interacting with one another. The second term accounts for the molecules mutually attracted and repellent forces. The constants 'a' and 'b' stand for the volume of the molecules and the attraction between them, respectively.

Eq. **( 2.17)** above was generalized by W.C Edmister by expressing the eight constants as a function of critical temperature, critical pressure and acentric factor (Machado et al., 2002):

$$\pi = \theta\rho + \left(B_0'\theta - A_0' - \frac{C_0'}{\theta^2}\right)\rho^2 + (b'\theta - a')\rho^3 + a'\alpha'\,\rho^6 + \left(\frac{c'\rho^3}{\theta^{\,2}}\right)(1+\gamma'\rho^2)^{-\gamma'\rho^2} \qquad (2.19)$$

where: π = P/Pc

θ = T/Tc

ρ = dRTc/Pc

The constants are functions of the acentric factor **ω**.

Using observed P-V-T data for thirteen hydrocarbons and carbon dioxide, Edmister and co. calculated pressures using both methods to compare their generalized equations to the original B-W-R equation. Based on their findings, the original B-W-R equation is typically only slightly less accurate than the generalized B-W-R equation (Machado et al., 2002).

In current studies, the generalized B-W-R equation has been used to analyse hydrogen and hydrogen-containing gas mixtures. The law of corresponding states that governs classical gases does not apply to quantum gases. As a result, without some minor adjustments to the critical constants, Eq.( 2.19) cannot be utilized directly for hydrogen, a quantum gas, or for mixtures containing hydrogen. This modification, as proposed by Gunn et al., is used in cases of critical conditions for quantum gases such as hydrogen:

Effective critical temperature,

$$T_C = \frac{T_C^{\circ}}{1 + (t_1/\mathrm{mT})} \qquad (2.20)$$

Effective critical pressure,

$$P_C = \frac{P_C^{\circ}}{1 + (t_2/\mathrm{mT})} \qquad (2.21)$$

Effective critical volume,

$$V_C = \frac{V_C^{\circ}}{1 + (t_3/\mathrm{mT})} \qquad (2.22)$$

where: $t_1 = 21.8°$ K

$t_2 = 44.2°$ K

$t_3 = -9.91°$ K

m = molecular weight of quantum gas, in this case hydrogen

T = absolute temperature of the system

This equation can be used to predict the behaviour of gases, especially at high temperatures and pressures and other thermodynamic properties such as equation of state, compressibility factor, and phase behaviour (Machado et al., 2002). B-W-R equation is not directly relevant to gas diffusion, it can be directly related to diffusion through the determination of thermodynamic properties. These properties, such as molar volumes, can be used to calculate diffusion coefficients using models such as the Chapman-Enskog theory or other approaches.

## 2.7. Hydrogen Loss in Caprock

On the case of predicting the hydrogen diffusion coefficient in different water saturated minerals, hydrogen diffusion was observed to be greatly influenced by the confined environment of the clay minerals and this in turn increased the diffusion coefficients due to porosity and permeability factors compared to their value in bulk water at the same thermodynamic conditions in which this confinement effect (wall effect of clay minerals) (Ghaedi et al., 2023). The findings imply that accurate caprock composition characterization is necessary for safe UHS and to avoid leaking. The major components and average pore size distribution are two parameters that can be crucial in figuring out the leaking potential.

Studies by (Xue et al., 2020) have also analysed the influence of $CH_4$ adsorption on diffusion and $CH_4$-water two-phase flow on sealing efficiency of caprock in underground energy storage. The infiltration of confined gas into the caprock because of the failure integrity shows the water saturation of the caprock changing significantly. The more gas diffusing into the caprock will significantly influence the gas sealing effect of the caprock and this is determined by the adsorption, this adsorption deformation affects the permeability of the caprock. The gas diffusivity and adsorption between the caprock matrix and the fractures will impact the gas flow in the caprock and the gas pressure distribution in the caprock. The thermodynamic effect of pressure in this process is then established, if any other gas is further introduced into the system. In addition, (Hoteit, 2011) gave further insight into the proper modelling of diffusion in fractured reservoirs, where he proposed the irreversible thermodynamic model. The theory of irreversible thermodynamics explains explicitly the chemical potential gradient as the driving force for diffusion (Hoteit, 2011). It is stated that diffusion occurs between two fluids(gases) with different chemical potentials and stops when the fluids become at chemical equilibrium (that is, equal chemical potentials). This idea aligns with the typical numerical

method, which assumes local chemical equilibrium and ignores diffusion at the simulation grid block level in isobaric and isothermal circumstances.

Lastly, a further development of the academic paper published by (Ghaedi et al., 2023)titled ´Hydrogen diffusion into Caprock: A semi-analytical solution and a hydrogen loss criterion` which has served as a base for my work. The investigation into the caprock was analysed using a one- and three-dimensional numerical models. The models considered the caprock and reservoir interaction and gas composition at the boundary. Based on chemical potential differences, hydrogen diffusion was studied while considering the impact of the hydrocarbon gas(es) already present in the caprock. In addition, a straightforward yet precise semi-analytical solution was suggested based on the parallels between the linked partial differential equations of diffusion and spontaneous imbibition processes. The presented results in the form of a semi-analytical solution can be used to predict cumulative hydrogen loss over time (Ghaedi et al., 2023). According to this analysis, hydrogen loss rises in direct proportion to the square root of time during semi-infinite conditions. The results obtained using diffusion fluxes demonstrated that if the presence of hydrocarbon gas in the caprock is disregarded, the hydrogen loss can be underestimated. According to the analysis, hydrogen loss is also directly proportional with the porosity of the caprock, the gas saturation of the caprock, the square root of the diffusion coefficient, and the square root of time. It is also directly correlated with the interface between rock and reservoir exposed to hydrogen while the presence of hydrocarbon gases indicated by $C_1$, $C_2$, $C_3$, $C_4$, $C_5$ effect on diffusion.

The work further gave some general equations and system description on which the working model was based upon giving some sets of solutions and the assumptions on which they are based. They are:

1) Analytical solution
2) Semi-analytical solution
3) Loss fraction criterion

## 2.8 Hydrogen Fraction Loss

Fick's second law of diffusion correctly predicts the $H_2$ ingress into the caprock over time. The $H_2$ concentration C *(z, t)* at a distance *z* from the caprock surface and at a time *t* is given by the generalized equation with initial and boundary conditions:

$$\frac{\partial C}{\partial t} = \frac{\partial}{\partial z}\left\{D(z,t)\frac{\partial C}{\partial z}\right\} \quad (2.23)$$

$Dc(z,t)$ is the diffusion coefficient and C *(z, t)* denoting the hydrogen profile. The Eq. (3.4) is solved under the assumptions that the diffusion coefficient $D_c$ *(z, t)* = D*(t)* and the boundary condition $C_i + \varphi(t)$ for $z = 0$ are time dependent, while the initial condition for $t = t_{ex}$, the exposure time concentration is a constant $C_i$. The mathematical terms that give a solution for the restriction can be formulated in the following way:

$$\frac{\partial C}{\partial t} = \left\{D(t)\frac{\partial^2 C}{\partial z^2}\right\}, \qquad z > 0, t > t_{ex}, \quad (2.24)$$

$$C(z, t_{ex}) = C_i, \qquad z \geq 0,$$

$$C(0, t) = C_i + \varphi(t), \qquad t \geq t_{ex},$$

$$\lim_{z\to+\infty} C(z,t) = C_i, \qquad t \geq t_{ex},$$

where: $\varphi(t)$ and $D(t)$ are continuous functions, $\varphi(t_{ex}) = 0$, $D(t) > 0$ everywhere for $t \geq t_{ex}$.In physical conditions, $C(z,t)$, and $\varphi(t)$, and $C_i$ are dimensionless, while the physical dimensions of $D(t)$ is lenght$^2$/time in m$^2$/year.

Due to thermodynamics, the diffusion coefficient $D_c$ is typically not a constant in the Eq.**( 2.23)** above but rather a function of concentration and the concentration is also dependent on space and time. The equation has an expression in a semi-analytical solution in integral form that is mathematically like the description of spontaneous imbibition (in a semi-infinite system). According to this semi-analytical solution, the position of a given concentration ($Z(C)$) depends on the concentration and is proportional to the square root of time ($t^{0.5}$), a constant $A_0$, and the concentration derivative of a function $F(C)$(Ghaedi et al., 2023):

$$Z(C) = 2A_0(C)t^{0.5} \quad (2.25)$$

The number of moles stored in the reservoir ($n_m$) is given by: Assuming a reservoir with a matrix porosity of $\phi_m$, area between the caprock and the reservoir exposed to hydrogen $A$, a vertical $H_2$ column height of H, a gas saturation of $S_g$, and an $H_2$ concentration of $C$ (assumed to be uniform in the reservoir and contacting the reservoir caprock boundary), the following values are given:

$$n_m = AH\phi_m S_g C \quad (2.26)$$

The total loss of $H_2$ in into the caprock can be expressed as:

$$n_i = 1.128\left(\frac{A_o}{A_{ocD}}\right) A\phi S_g C\sqrt{\overline{D}}\sqrt{t} \quad (2.27)$$

To evaluate the loss fraction of the stored hydrogen when diffusion has occurred over time, we can apply:

$$LF = \frac{n_i}{n_m} = 1.128\left(\frac{A_o}{A_{ocD}}\right)\frac{S_g\phi C_{cap}}{S_g\phi_m C_{res}}\frac{\sqrt{\overline{D}}\sqrt{t}}{H} \quad (2.28)$$

where: $n_i$ the number of moles of $H_2$ in the caprock i.e., the total loss of $H_2$

$\frac{A_o}{A_{ocD}}$ a function of diffusion coefficient skewedness, with a magnitude close to 1

$C_{cap}$ the concentration diffused into the caprock, $C_{res}$ concentration contained in the reservoir.

$\overline{D}$ mean diffusion coefficient, a function of the activity corrected diffusion coefficient.

To address the knowledge gap in the numerical simulation of $H_2$, this research will investigate the P-T thermodynamic properties, consider the presence of hydrocarbon gas(single and binary component) in the caprock and investigate the relationship between boundary concentrations $C_{i*}$($H_2$ concentration above the caprock interface) and $C_{i0}$ ($H_2$ concentration below the caprock in the reservoir) at different reservoir pressures and temperatures (see Fig 3.2 for detailed schematic representation). Also, I will be investigating diffusion time, changing porosity and permeability of the caprock, presence of different hydrocarbon gases in the caprock and finally changing temperature and pressure at different depths of the storage reservoir.

# Chapter 3: Methodology

## 3.1 Introduction

This chapter explains the methodology applied to the numerical simulation of hydrogen stored in the depleted gas reservoir. The simulation was discussed beginning with the numerical simulation theory of diffusion using the software as presented in the model system and followed by the assumptions made on the model while performing the analysis. The model described and the information about the reservoir will be processed using the ECLIPSE 300 software compatible with the compositional simulation.

## 3.2 ECLIPSE Software

The ECLIPSE reservoir simulator suite is a commercial product of SLB (formerly Schlumberger). it consists of two distinct simulators: ECLIPSE 100, and ECLIPSE 300. There are three operating modes for ECLIPSE 300: implicit, IMPES, and adaptive implicit (AIM). For this work, we will be using ECLIPSE 300 compositional simulator and Peng-Robinson equation of state used to model the fluid flow properties.

ECLIPSE 300 is one of the options for reservoir simulation used in modelling black oil and compositional data files on the software. Modelling is done using feed-forward calculation and Equation of state (EOS). Additionally, it offers a vast array of additional capabilities, such as the capacity to enhance oil recovery (EOR), recover coal and shale gas, mimic advanced wells, and store $CO_2$, and can be configured to model UHS as adopted in this work.

This software thoroughly explains compositional changes and reservoir fluid phase behaviour. This numerical simulator was employed to conduct the current simulation study to investigate the diffusivity process involving hydrogen. With specific diffusion coefficients, set boundaries and conditions. More importantly, it supports the comparison of the two diffusion models, a potential chemical gradient and molecular diffusion driven by concentration (B.C Craft, 2014), which is one of the objectives of this study

### 3.2.1 Modeling Approach in Eclipse Simulator

The reservoir model description is a 1D reservoir in the Z-cartesian plane with a chemical potential activity driven diffusion. This plane was chosen to help in the proper visualization of the diffusivity spread from the reservoir into the caprock. To predict diffusion using the reservoir compositional simulator, we can make use of two diffusion models, where diffusion flux as in Eq. **( 3.5)** is either produced by the concentration or chemical potential gradient, both models allow for the setting of Nc diffusion coefficients under the assumption that they are constant (where Nc is the number of components available in the datafile model) and support the effective diffusivity model. The composition of the mixture steadily shifts as the simulation of the diffusion process advances. As the pressure increases, composition changes can create a significant change in how the mixture behaves (Shafikova, 2013) and the varying reservoir pressure can also be derived as well as the temperature from Eq. **(** 2.8) and ( 2.9). The Eclipse 300 simulator requires a single, distinct diffusion coefficient for each component to mimic diffusivity flux.

In addition, we will also simulate diffusion varying the different composition at the section with the $H_2$, $C_1$, $C_2$, $C_3$, $C_4$, $C_5$ components denoting hydrogen, methane, ethane, propane, butane, and pentane, respectively. The porosity of the caprock can also be varied to investigate the rate of diffusion over a period. The datafile sections can also be altered to depict the reservoir depth at this can also model the pressure and temperatures at that depth, aiding the understanding of the thermodynamic effect of these properties to the rate of diffusion (concentration profile).

$H_2$ diffuses from the reservoir through the caprock from low $R_v$ (vaporized oil-gas ratio) to high $R_v$ region. The molar amount of gas is given as:

$$M_{gas} = \frac{S_g \rho_g}{B_g MW_g} \qquad (3.1)$$

The gas total molecular concentration C is given by:

$$C_g = \frac{S_g}{B_g}\left(\frac{\rho_g}{MW_g} + \frac{R_v \rho_o}{MW_o}\right) = \frac{S_g \rho_g}{B_g MW_g}(1 + R_v F) \qquad (3.2)$$

$$F = \frac{\rho_o MW_g}{\rho_g MW_o} \qquad (3.3)$$

From this, for any two cells, the diffusive flow is proportional to the cross-sectional area between the cells and inversely proportional to the distance between them. Equilibrium in diffusion is obtained when the component chemical potential is equal to the gravity potential. Eclipse calculates the diffusive flow from the following expression (in the gas-in-gas case) as:

$$F_{diff} = T_d D_{gg} S_g B_g (x_i - x_j) \quad (3.4)$$

where: $T_d$= diffusivity, $D_{gg}$ = gas-in-gas diffusion coefficient

$S_g$ = gas saturation

$B_g$ = gas formation volume factor

$\rho_g$ = surface density of gas

$\rho_o$ = surface density of oil

$MW_g$ = molecular weight of gas

$MW_o$ = molecular weight of oil

$R_v$ = vaporized oil-gas ratio

$x_i, x_j$ = the gas mole fraction in the gas phase in cells i and j.

## 3.3 Reservoir model and Assumptions

As shown in Fig 3.1, the depleted gas reservoir in consideration has already pre-defused natural gas hydrocarbon components such as methane in its caprock. When it is used for seasonal $H_2$ storage, the diffusivity value of hydrogen in reservoir conditions which is less than that of methane will cause an upward movement of $H_2$ molecules into the pores of the caprock. The free-phase gas leakage (the uncontrolled release or escape of gas in its gaseous phase from the reservoir) through faults or fractures was disregarded because it was assumed as uncommon in the natural gas reservoirs. Also, the dissolution of gas in the water that occupies the pores of the caprock, and the underlying aquifer was also neglected in this study as water in caprock was not considered. Due to the lower density of hydrocarbons compared to the fluids and rocks around them, it tends to move closer to the earth's surface. The movement of hydrocarbons along long distances is referred to as hydrocarbon migration. Some variables, including the permeability of the rocks, pressure and temperature gradients, and the presence of faults or

fractures in the rocks, all affect the migration of hydrocarbons. When $H_2$ gas is injected into the reservoir for storage, over time it shows a trend of molecular diffusion into the caprock influenced by the chemical potential. This is also because of the concentration gradient of gas from a higher concentration to that of a lower concentration gradient i.e., the differences between the fugacity in the caprock and reservoir.

The model in this work was adopted as a 1-D because it is easier to numerically simulate and mimic the reservoir activities being considered also the presence of the previously migrated hydrocarbon gas was considered in this work. Prior desired temperatures and pressures of 50°C and 200 bars respectively were assumed with $H_2$ in the reservoir and only hydrocarbon gas in certain total mole percentages of the caprock depending on the PVT conditions. A caprock of 20m in the X and Y dimension (contact area A in contact 400$m^2$) length in the Z-direction of 500m and fine grid size of 1m was considered to help determine the molar density in the gas phase (moles per reservoir volume of $H_2$ diffusing into the caprock). Also, a reservoir block size of 10 m in Z direction was used to obtain a semi-finite condition for $H_2$ diffusion into the caprock. To achieve a constant concentration border, the $H_2$ concentration in the reservoir and below the contact between the caprock and the reservoir were also maintained constantly. The PVT conditions of the caprock determine the amount of water and gas phase present in the caprock and they are hence set to a relative permeability of zero value because of the impermeability of the caprock. The uniform caprock porosity of 10% and an assumption that the thickness hence porosity of the reservoir is ignored. In order to correctly define the reservoir temperature and pressure, a surface temperature of 15 °C and temperature gradient of 0.033°C/m was adopted alongside a surface pressure of 1.01323bar and pressure gradient of 0.1bar/m was also considered alongside varying reservoir depths stated in Eq.( 2.8)( 2.9).

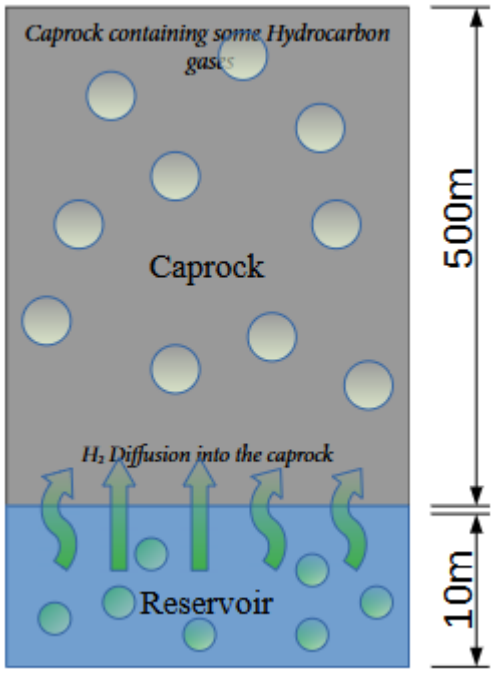


**FIG 3.1**: Schematic representation of the reservoir model showing the present hydrocarbon gas and $H_2$ diffusion.

The boundary concentration ±1 m above and below the caprock is important to estimate the scale of $H_2$ loss into the caprock. This simulation was performed at varying temperatures and pressures and the change in fugacity of $H_2$ in the reservoir and caprock resulted in the molecular diffusion. The $H_2$ concentration is constant when this measure of the difference between its chemical potential in the reservoir-caprock system and its chemical potential in its hypothetical ideal-gas standard state at the same temperature comes to an equilibrium.

In the application of gas diffusion from reservoir to the caprock, components with different composition, such as $C_1$ to $C_5$, were used to identify lighter components, such as $C_1$, and heavier components, such as $C_5$. The caprock above the reservoir is the membrane for diffusion with some thickness. Some relationships can be stated as follows: (1) A thicker porous membrane reduces the rate of diffusion. (2) Increased surface area of the membrane increases the rate of diffusion. (3) The greater the distance that the gas must travel, the slower the rate of diffusion. (4) Higher temperatures increase the energy and therefore the movement of the molecules, increasing the rate of diffusion. Lower temperatures decrease the energy of the molecules, therefore decreasing the rate of diffusion (Widyanita et al., 2021). The numerical simulation is implored to understand the role of the impact of the diffusion concept and the thermodynamic

effect on the stored hydrogen as it diffuses. The fundamental equation of a reservoir model for this kind of problem is utilizing the modern theory which assumes that molecular diffusion is purely driven by the chemical potential of the system (Muhammed et al., 2023). $H_2$ diffusion process can be accurately represented by a flux-based chemical potential gradient:

$$J_i = -CD_i^a y_i \frac{1}{RT}\frac{\partial \mu_i}{\partial Z} \quad (3.5)$$

Due to the elongated duration of contact between the caprock and gas as earlier mentioned, the presence of hydrocarbon gas in the caprock is considered in the description of this model. The flux of a component *i* (i.e., molecular flux of component *i*) per unit area accessible to the flow is given as Ji ($\frac{mol}{s\ m^2}$) and expressed as:

$$J_i = -CD_i^a y_i \frac{\partial (lnf_i)}{\partial Z} = -CD_i^a y_i \frac{\partial (lnf_i)}{\partial (lny_i)} \frac{1}{y_i}\frac{\partial y_i}{\partial Z} = -CD_i^a \frac{\partial (lnf_i)}{\partial (lny_i)} \frac{\partial y_i}{\partial Z} \quad (3.6)$$

$H_2$ will naturally seep into the caprock from the top of the reservoir, and this is due to its small size and low molecular density. We can assume that the interface between the reservoir and the caprock is at $Z = 0$. The composition $yi_0 = yi\ (Z = 0^-)$ and total reservoir molar concentration $C_0 = C\ (Z = 0^-, t)$ are then taken into consideration at $Z = 0$. With the $H_2$ concentration at zero and the hydrocarbon content at non-zero, the caprock's original makeup $(Ci, _{ini})$ is known. It is assumed that the system is semi-infinite (i.e., the initial concentration is obtained as Z goes to infinity). In summary, the conditions can be listed and represented schematically in Fig 3.2

$$Ci = Ci, ini, Z > 0, t = 0 \text{ [Initial Condition in the Caprock ]} \quad (3.7)$$

$$Ci = Ci0, Z = 0-, t > 0 \text{ [Caprock} - \text{Reservoir Interface]} \quad (3.8)$$

$$Ci = 0, Z = \infty, t > 0 \text{ [Far from Caprock} - \text{Reservoir Interface]} \quad (3.9)$$

where $C_{i0}$ is the $H_2$ concentration below the caprock in the reservoir.

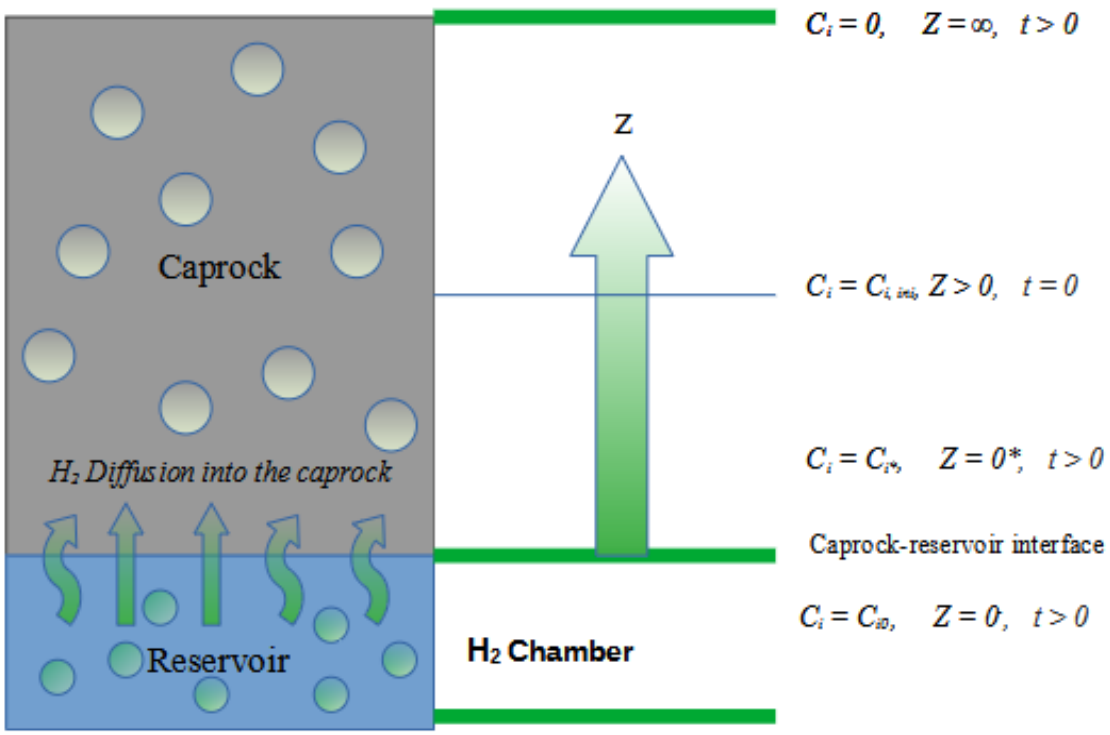


**FIG 3.2**: $H_2$ diffusion through caprock modelling a linear diffusion (modified from **(GHAEDI ET AL., 2023)**, Fig 3.)

From available studies, the continuity of chemical potential of a gas after passing through a medium does not necessarily correspond to continuity of concentration, we will have a composition $C_{i*\ as}$ the boundary concentration just after the caprock which may differ from $C_{i0}$ (Ghaedi et al., 2023). The boundary conditions for $C_{i*}$ can be expressed as:

$$Ci = Ci*, Z = 0+, t > 0 \text{ [Caprock Reservoir Interface]} \quad (3.10)$$

The semi-analytical solution states that the position of a given concentration $(Z(C_i))$ is proportional to the square root of time ($t^{0.5}$), a constant $A_0$ and the concentration derivative of a function $F(C_i)$ depending on concentration. mathematically represented as:

$$Z(C_i) = 2A_0F'(C_i)t^{0.5} \quad (3.11)$$

The semi-analytical solution assumes that for $H_2$ diffusion to the caprock the total concentration in the system is constant. The concentration component ($C_i = Cy_i$) can then be rewritten as:

$$J_i = -CD_i^a \frac{\partial(lnf_i)}{\partial(lny_i)} \frac{\partial C_i}{\partial Z} \quad (3.12)$$

$J_i$ from Eq.) can be further expressed by factoring the Fick's first law, where diffusion coefficient is the only parameter to consider other than the concentration gradient. We then have:

$$J_i = -CD_i \frac{\partial C_i}{\partial Z} \text{ , where } D_i = D_i^a \frac{\partial(lnf_i)}{\partial(lny_i)} \quad (3.13)$$

In the above equation, $D_i^a$ only depends on the pores and fluids configuration in the porous medium. A crucial point to note is then how the term $\frac{\partial(lnf_i)}{\partial(lny_i)}$ affects the $H_2$ loss through the caprock. The term $\frac{\partial(lnf_i)}{\partial(lny_i)}$ only depends on the thermodynamic of the system and in a condition where both temperature and pressure are constant, it varies only with gas composition. Thus, its dependency can be expressed by $C_i$ and at low pressures $\frac{\partial(lnf_i)}{\partial(lny_i)} \longrightarrow 1$. Then, the flux of chemical and potential driven diffusion become equal (Ghaedi et al., 2023).

## 3.4 Simulation data

The data used for analysing the results and plots from the simulation was obtained from the simulators mentioned earlier. The data gave BMLSC (moles per pore volume), RCGMI (molar amount), time in years. BMLSC helped in the derivation of the $H_2$ gas concentration per caprock volume in Kmol/m$^3$ by dividing by gas saturation $S_g$ as obtained from running an analysis with PETREL, RCGMI was used in obtaining the cumulative $H_2$ loss to the caprock by dividing the area of caprock in contact with $H_2$ and lastly the square root of time was derived from the time in years. Plotting the values obtained as the gas concentration in the caprock against time will yield the result describing the mole amount of $H_2$ gas that must have diffused into the caprock and predict the time taken to be diffused. The data obtained from dividing the RCGMI with the area is used to plot for predicting the cumulative amount lost in the caprock against the square root of time which also confirms the analysis of Eq. (2.28**( 2.25**). Further data for analysis were drawn from these basic calculative derivations made from the dataset from the software used.

# Chapter 4: Results and Discussions

## 4.1. Introduction

The numerical modelling approach remains one of the best tools that can help define the reservoir model. In this research, we have adopted a fully implicit compositional simulation approach and Schlumberger's commercial simulator Eclipse 300 was combined to simulate a UHS site. The fluid characteristics of UHS were modelled using the Peng-Robinson equation of state, which has already been employed by other authors and researchers. The simulator helped in defining the diffusion properties, mirroring actual reservoir conditions and helping to solve the complexities presented in understanding gas migration, especially as presented by the diffusion of $H_2$. The $H_2$ diffusion is driven by a chemical potential gradient which has been simplified as the concept of diffusion into the caprock. In the previous chapters, theoretical explanations and literature studies of basic principles have been presented and but the idea here is to critically analyse these studies and theories by modelling the concept of molecular gas migration driven by the chemical gradient into the caprock. We will also analyse and present results by varying different hydrocarbons present in the caprock, the porosities of the caprock and finally the PVT values to visualize their effect on the thermodynamics of hydrogen diffusion process.

The sensitivity analysis will present the following effects on $H_2$ diffusion by varying in the HC component present in the caprock including multiple gases (binaries), effect of P-T gradients and effects of porosity induced rate. Further analysis will also be performed on the comparison of the activity corrected diffusion coefficients with the calculated diffusion coefficient value estimated from the Sigmund correlations, Wilke-Chang correlations, and that of Belery and da Silva.

## 4.1 Effect of Pressure on $H_2$ diffusion

### 4.1.1 Caprock Saturated with Single Gas

The variation of pressure influences $H_2$ diffusion. The numerical simulation performed on the reservoir model has the temperature set at 50°C and variation of pressure was set increasingly

from 50 bar, 100bar, and 150 bar with respect to the relationship of depth and surface pressure of 1.01325 bar, methane at a gas fraction $ZC_1$ at 1, and porosity at 1%.

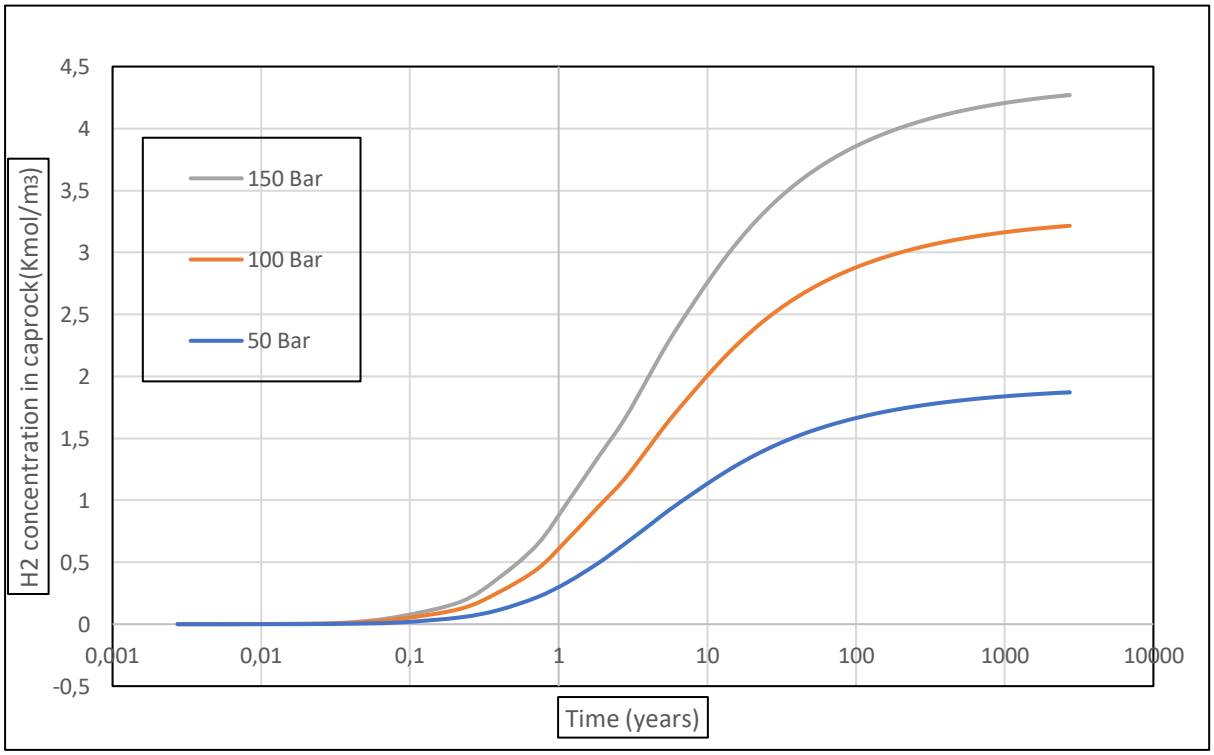


**FIG 4.1:** Effect of varying pressure on concentration rate of $H_2$ diffusion in the caprock

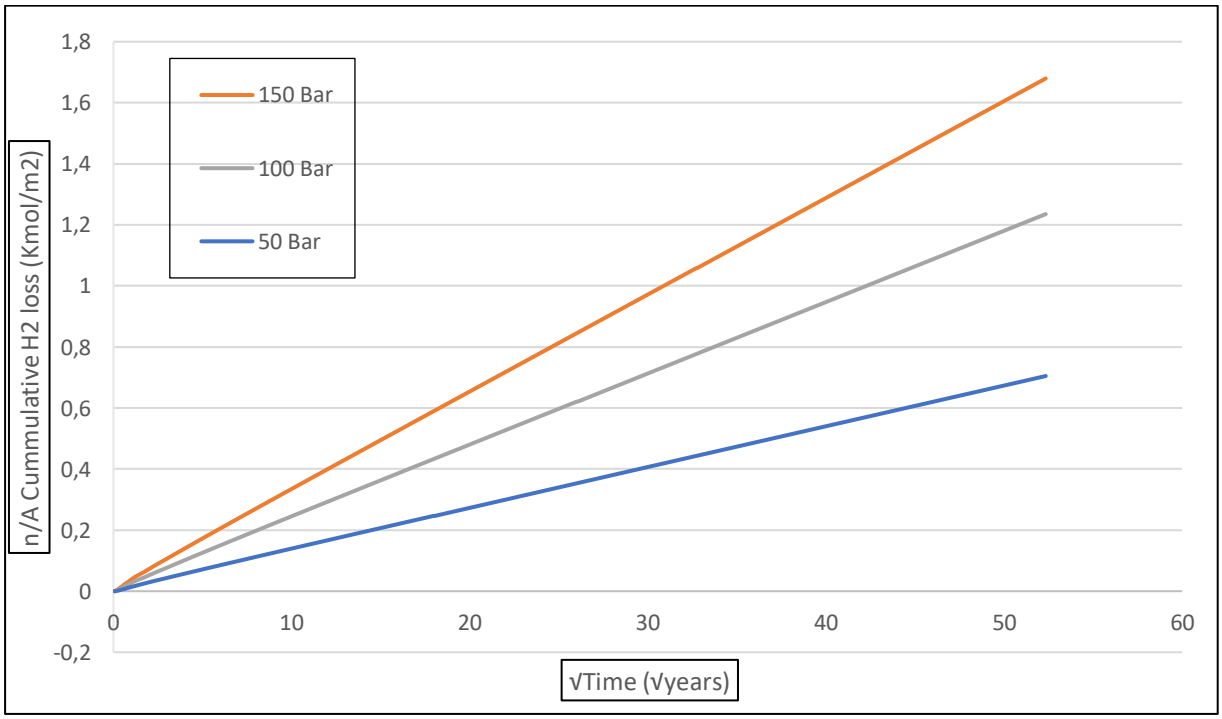


**FIG 4.2** Cumulative loss on varying pressure on $H_2$ loss in the caprock

The results obtained in Fig 4.1 shows that $H_2$ concentration profile was seen to decrease from the peak concentration values of 4.3 Kmol/$m^3$ through the caprock as the pressure varies from higher to lower. This validates the study that concentration increases with pressure increase and that increase in pressure is directly proportional to the rate of diffusion. When the pressure in a gas reservoir increases, the $H_2$ gas molecules become more closely packed together thereby experiencing an increase in the chemical potential near the caprock. This increased pressure results in a higher concentration of gas molecules in the caprock pores. The increased pressure also leads to higher kinetic energy which enables the gas molecules to move more randomly, which increases the rate of diffusion. In contrast, the gas molecules travel more slowly and with less kinetic energy when the pressure is reduced, their diffusion rate thus declines. The effective cumulative loss is also analysed to be a small fraction of the total $H_2$ contained in the reservoir, but still the effect of the pressure variation is not to be underestimated in UHS process.

### 4.1.2 Caprock Saturated with multiple Gases

Hydrocarbon binaries used for this analysis were methane and pentane. Based on studies, $C_1$ and $C_5$ are two crucial HC components of natural gas that can properly simulate the binary behaviour of HC in reservoir conditions, and this binary system ($C_{1,5}$) is frequently used to represent a mixture of them. The behaviour of this binary system can be used to simulate natural gas reserves with various compositions. The variation of pressures from 50 bar,100 bar, 150 bar and at temperature 50℃.

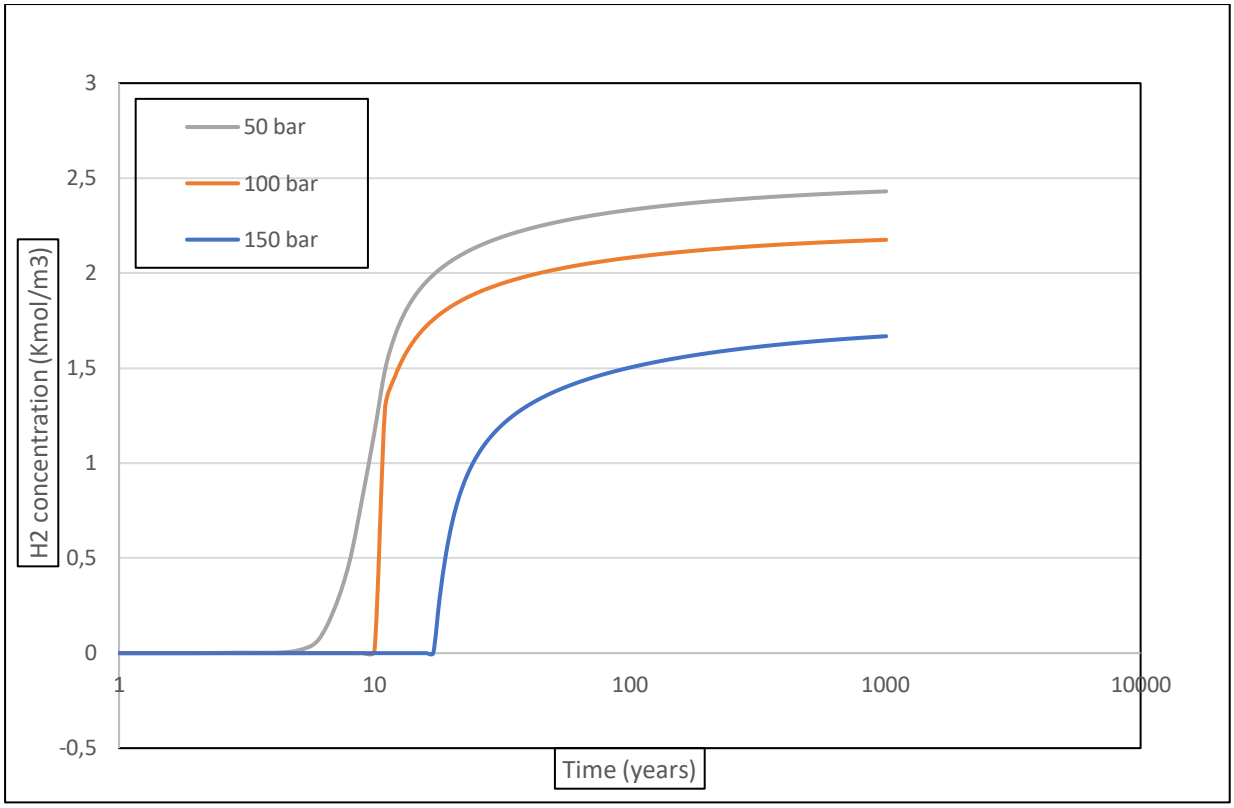


**FIG 4.3:** Effect of multiple hydrocarbon gas on concentration rate of $H_2$ diffusion in the caprock.

The results in Fig 4.3 shows that on applying a high pressure on low temperature, binary HC component cross-phase to oil is possible. At 150 bars, a constant concentration was observed over a period and that further explains the results of the cumulative loss in Fig 4.4. at increasing pressure and reduced temperature for a multiple gas condition, it is observed that loss into the caprock decreases.

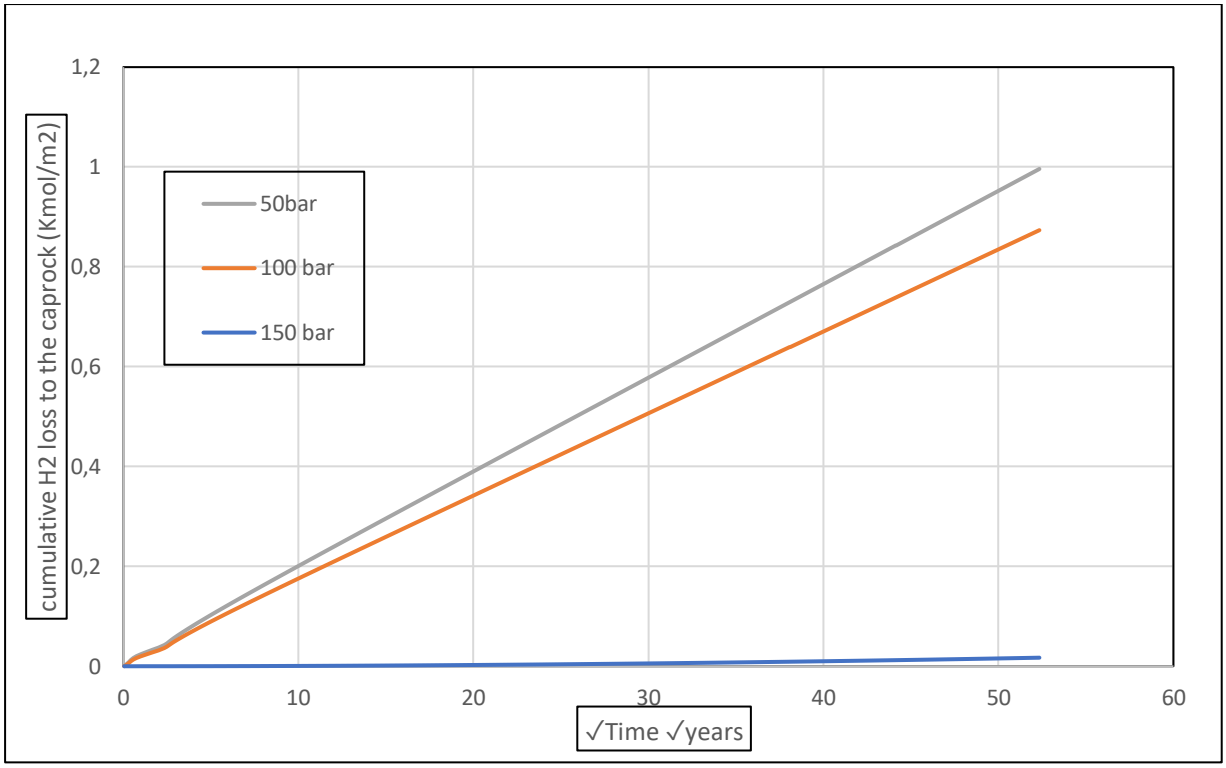


**FIG 4.4:** Cumulative loss of $H_2$ on hydrocarbon binary component in the caprock.

At pressure 150bar and 50 ℃ temperature, the gas saturation $S_g$ 1m above the caprock was observed to be very low at value 0.002. indicating low saturation to the caprock on the effect of increased pressure and low temperature.

## 4.2 Effect of Temperature on Hydrogen Diffusion

### 4.2.1 Caprock Saturated with Single Gas

To properly understand this effect, a numerical analysis was performed setting the reservoir pressure at 100 bar, porosity at 10 % and butane C4 contained in the caprock. The temperature variations of 50℃, 90℃, and 150℃ were applied to the model. The results show the relationship between concentration in Kmol/$m^3$ and time taken to diffuse in years in Fig 4.5, also the amount lost or the cumulative loss to the caprock as a square root of time Fig 4.6.

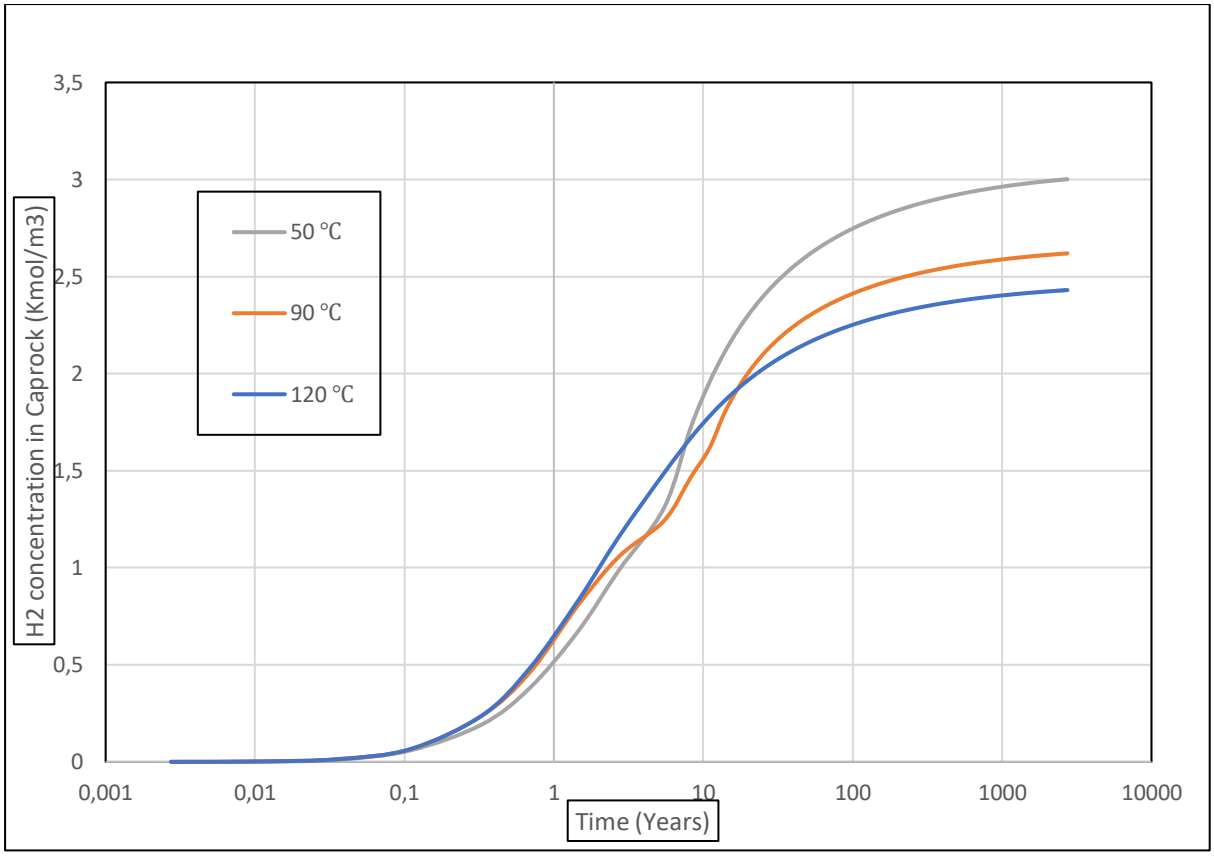


**FIG 4.5:** Effect of varying temperature on concentration rate of $H_2$ diffusion in the caprock

From the results and analysis, Fig 4.5 indicates that at higher temperatures, there is a decrease in the upstream concentration of $H_2$. This is as a result of temperature on the equilibrium of the gas phase and the dissolved phase present in the surface of the caprock. The increase in temperature leads to an increased tendency for the gas molecules to escape from any dissolved and enter the gas phase. As a result, more molecules transition from the dissolved state to the gas phase with increased energy and collision, causing a decrease in the concentration of $H_2$ in the dissolved phase. This will in turn result in a decreased cumulative loss to the caprock with respect to time as seen in fig 4.7.

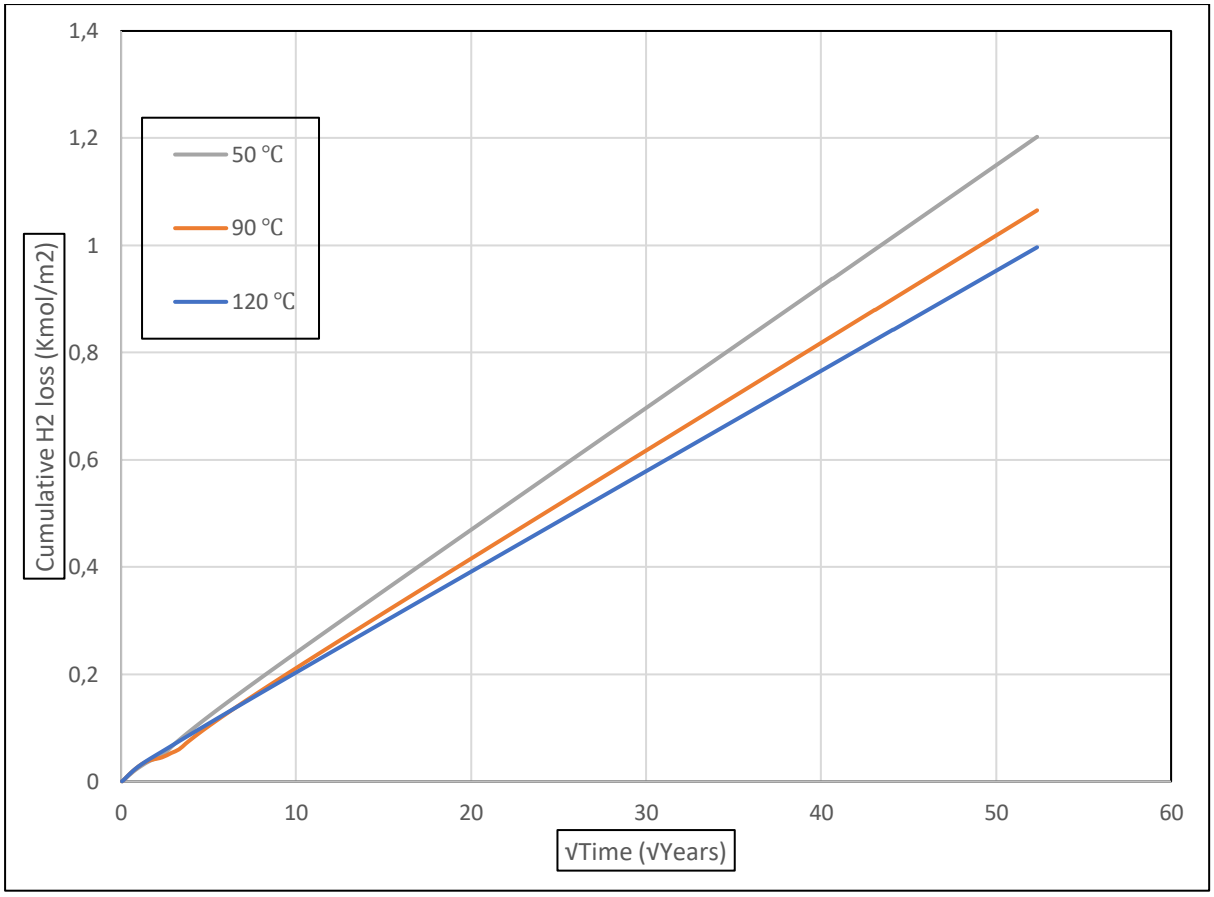


**FIG 4.6:** Cumulative loss on varying temperature components in the caprock

The results from Fig 4.6 show the cumulative loss to the caprock at increased temperature. The effective loss amount is a small fraction compared to the total amount in the reservoir. The total amount of 88% was analysed after a period of 30 years. The effect of temperature on diffusion is not to be underestimated hence the effective consideration in UHS.

### 4.2.2 Caprock Saturated with multiple Gases.

As seen in Fig 4.7, the effect of multiple HC gas saturation at varying temperatures shows that temperature increase can lead to cross-phase conditions but at high temperature of 150°C, the cross-phased component will readily sip away from the pores of the caprock giving paces for diffusion to take place. However, at a very low rate as seen from the concentration profile and from Fig 4.8 which gives a very low cumulative loss and a decreased upstream concentration of $H_2$ in the caprock.

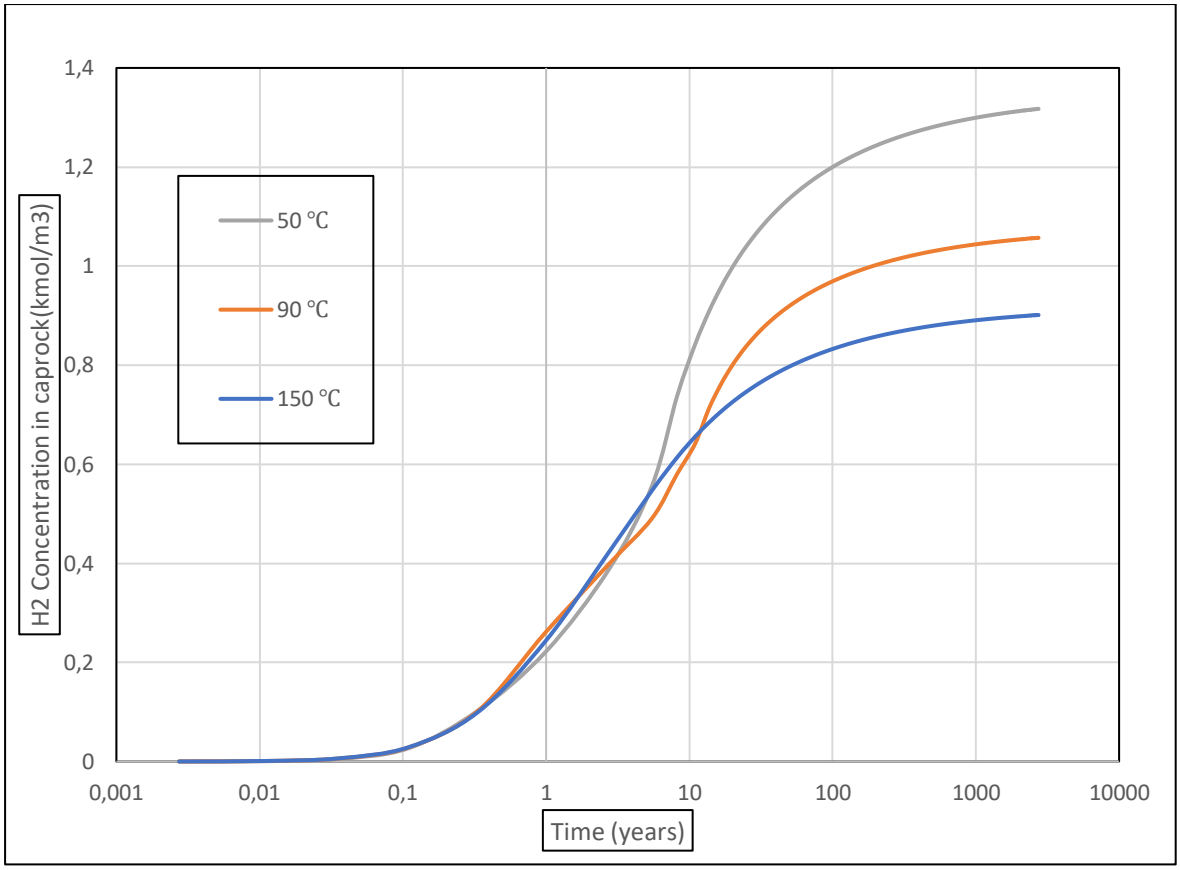


**FIG 4.7:** Effect of multiple gas saturation on concentration rate of $H_2$ diffusion in the caprock

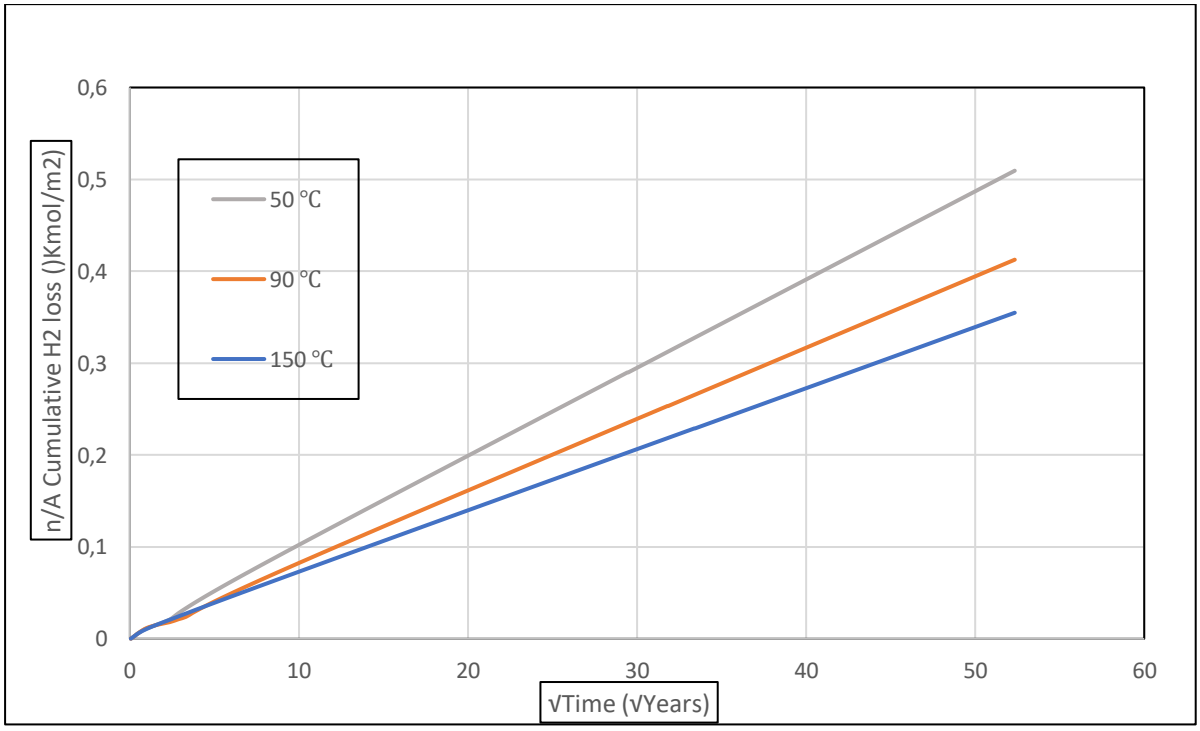


**FIG 4.8:** Cumulative loss on multiple gases in the caprock at varying temperatures.

The cumulative loss at varying temperatures decreases as temperature increases. In the effect of multiple HC gases (binaries), the heavy binaries showed some effect with the decrease in the peak cumulative loss of 0.51 Kmol/m$^2$ as compared to that in Fig 4.6 where the loss can be seen to be at 1.2 Kmol/m$^2$. As visualized from the software Petrel, gas saturation $S_g$ value of 0.88 was observed +1m above the caprock at 50℃. This also supports the results that temperature increase has a great effect on $H_2$ diffusion at different densities of binary HC present in the caprock.

## 4.3 Effect of Hydrocarbon gas component in the caprock on $H_2$ diffusion

The simulation of the effect of varying hydrocarbon components on diffusion is seen by the build-up of the concentration diffused into the caprock in Kmol/m$^3$. The model used has pressure at 100 bar, temperature of 50 ℃, constant $D_i^a$, porosity values at 1 % while varying the different hydrocarbon component from C1 through C5. The effect as shown gives a clear description of this effect on diffused gas concentration in the caprock and the cumulative loss into the caprock.

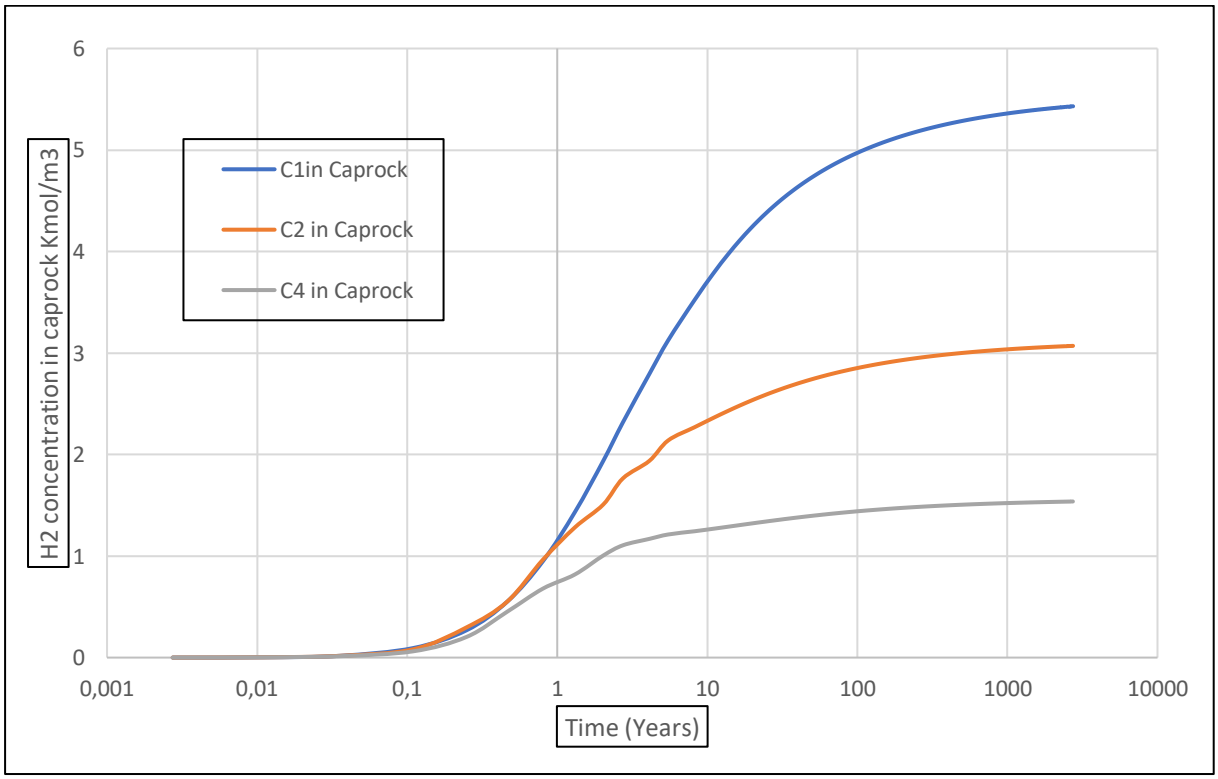


**FIG 4.9:** Effect of varying hydrocarbon component on concentration rate of $H_2$ diffusion in the caprock.

The results in Fig 4.9 show that the concentration of $H_2$ at the caprock decreased when HC components moved from less HC dense to denser HC components. It is observed that at C1 to C5 variation, the concentration profile decreases from 5.5 Kmol/$m^3$ for C1 to 1.5 Kmol/$m^3$ for C5. This is valid because the caprock pores are filled with denser HC that may contain oils, decreasing permeability. The $H_2$ molecules tend to move from regions of higher chemical potential to regions of lower chemical potential. This movement aims to balance the chemical potential throughout the reservoir and reach a state of equilibrium. When hydrocarbon molecules are dissolved in the pores of the caprock, they contribute to the overall chemical potential of the system in those caprock. The dissolved hydrocarbons create a higher chemical potential compared to that of the reservoir that do not contain dissolved hydrocarbons. As a result, the concentration gradient of $H_2$ diffusing through the caprock is affected. The concentration gradient, which is also a factor for this diffusion, affects molecules as they tend to move from regions of higher concentration to regions of lower concentration. However, the presence of dissolved hydrocarbons creates a localized region of higher concentration and higher chemical potential in the caprock. The diffusion of molecules through the caprock is hindered because it would involve moving from regions of lower chemical potential to regions of higher chemical potential (due to the dissolved hydrocarbons). This is energetically unfavourable and thus decreases the rate of diffusion through the caprock.

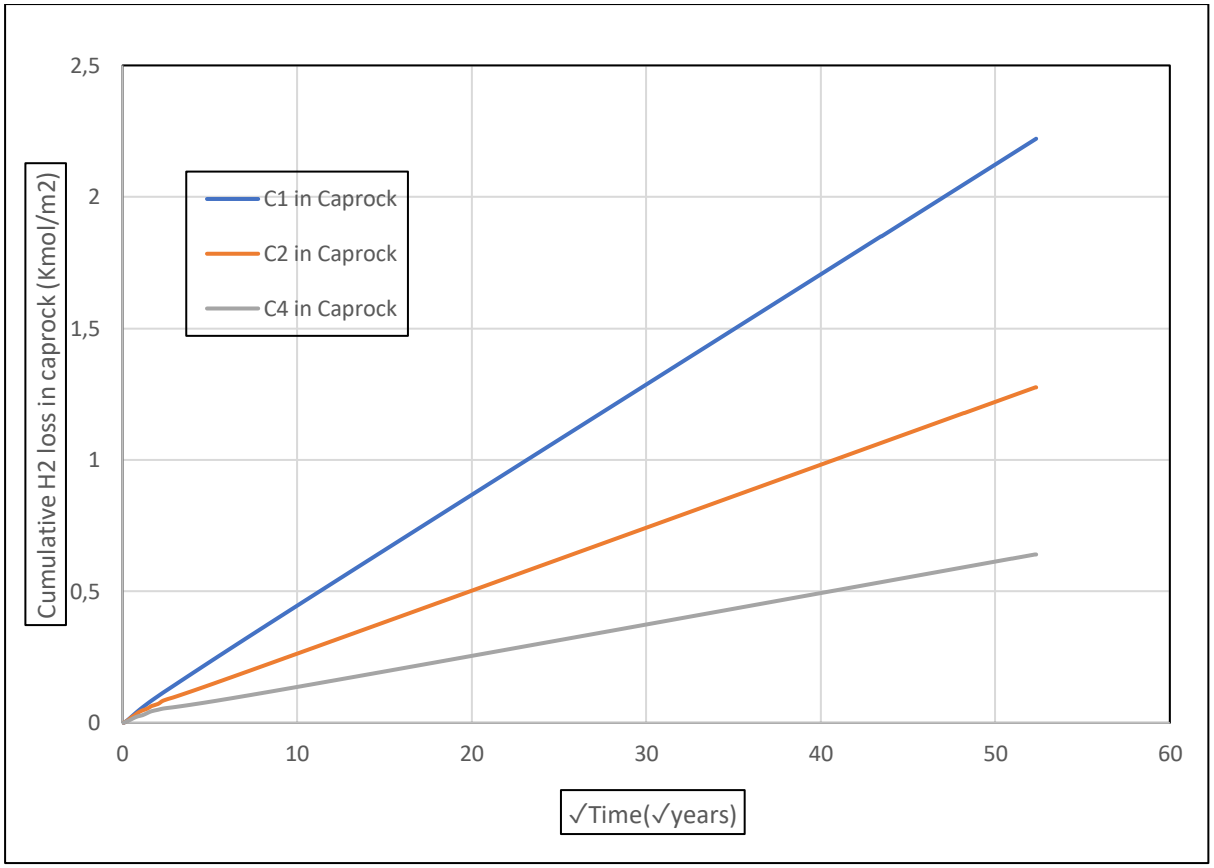


**FIG 4.10:** Cumulative loss on varying hydrocarbon component in the caprock

As shown in Fig 4.2, the cumulative loss at varying HC component indicates that there is also a decreasing cumulative loss to the caprock. The loss as compared to the reservoir retention varied from 76% for C1 to 89% for C5.

## 4.4 Effect of porosity on $H_2$ diffusion

The simulation of the effect of varying porosity on diffusion is seen by the build-up of the concentration diffused into the caprock in Kmol/m$^3$. The model used has pressure at 100 bar, temperature of 50 °C, C1($Z_{c1}$), constant $D_i^a$ while varying porosity values from 1 %, 5 %, and 10 %. The effect in Fig 4.1 shows a comparison and diffusion curve indicating concentration build-up with respect to time between different values of porosity as stated earlier.

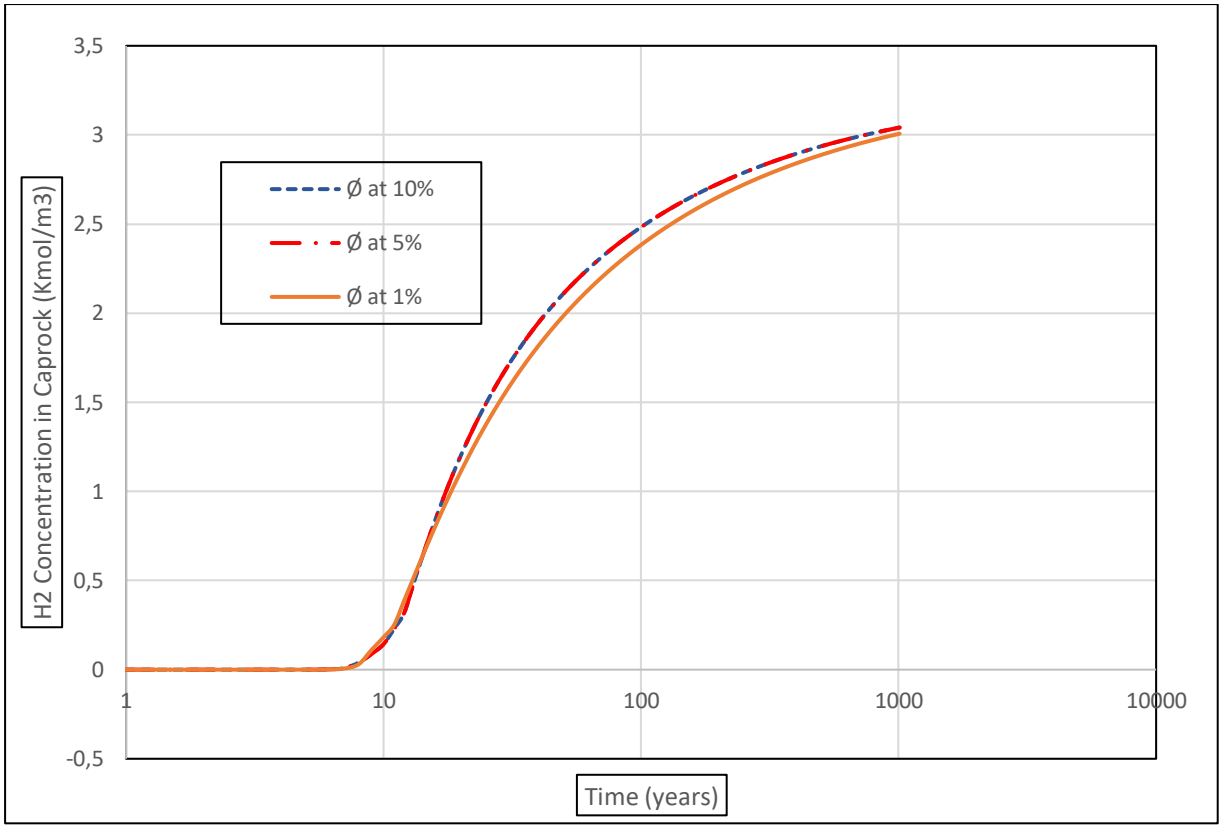


**FIG 4.11:** Effect of varying porosity on concentration rate of $H_2$ diffusion in the caprock.

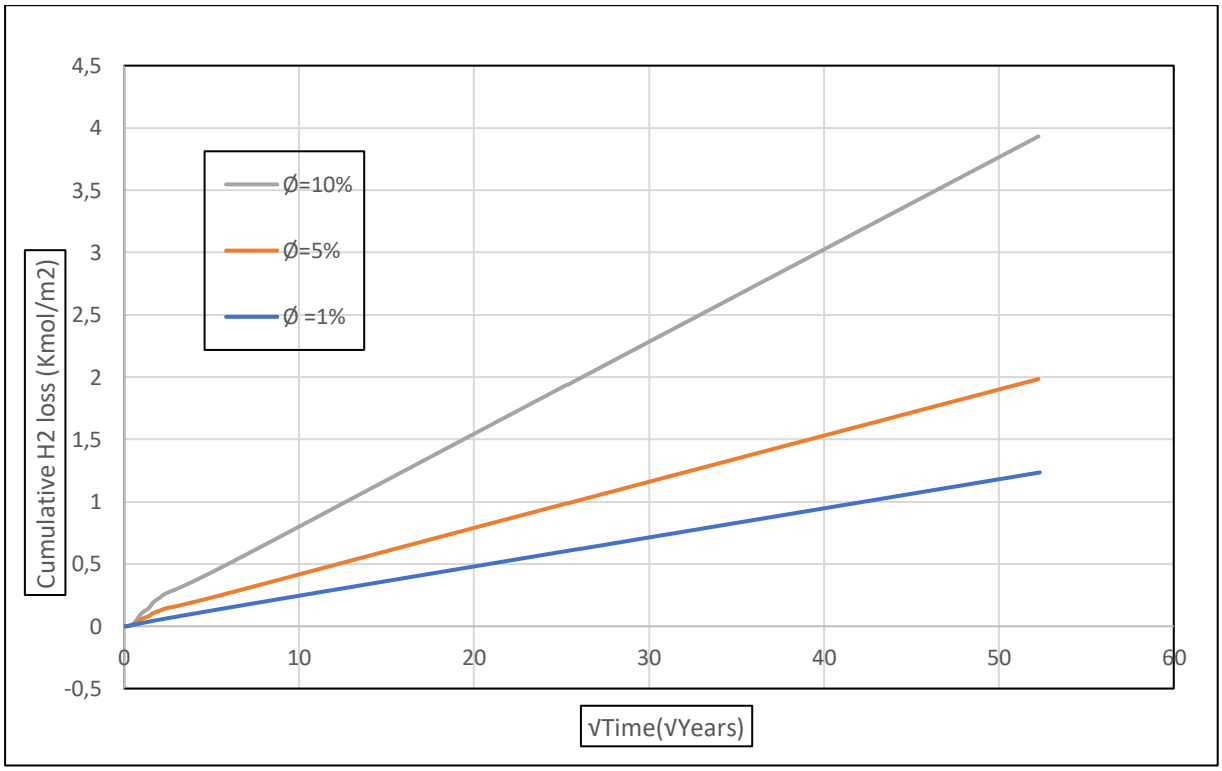


**FIG 4.12:**Cumulative loss on varying porosity of the caprock.

From previous studies, it has been observed that shale caprock has low permeability and hence low effective porosity. It is observed in Fig 4.1, that at every instance of varying porosity, the ratio of the $H_2$ concentration to the available pore volume is almost the same with some minor deviations in the concentration profile. As seen in Fig 4.12, the loss is directly proportional to the square root time and Eq. (2.30**( 2.27**) shows that the amount of loss of is directly proportional to the porosity of the caprock. $H_2$ storage in UHS with low porosity caprock can therefore be recommended for the UHS.

## 4.5 Effect of Diffusion correlation on $H_2$ diffusion

Simulation of the diffusion coefficient $D_i^a$ effect on diffusion was properly visualized by the concentration diffused into the caprock in Kmol/m$^3$. The model used has pressure at 100 bar, temperature of 50 °C, C1($Z_{c1}$), and porosity 0.01. The effect in Fig 4.13 shows a comparison between the model's diffusion coefficient $D_i^a$ $10^{-9}$m$^2$/s and that suggested by the $H_2$ diffusion correlations.

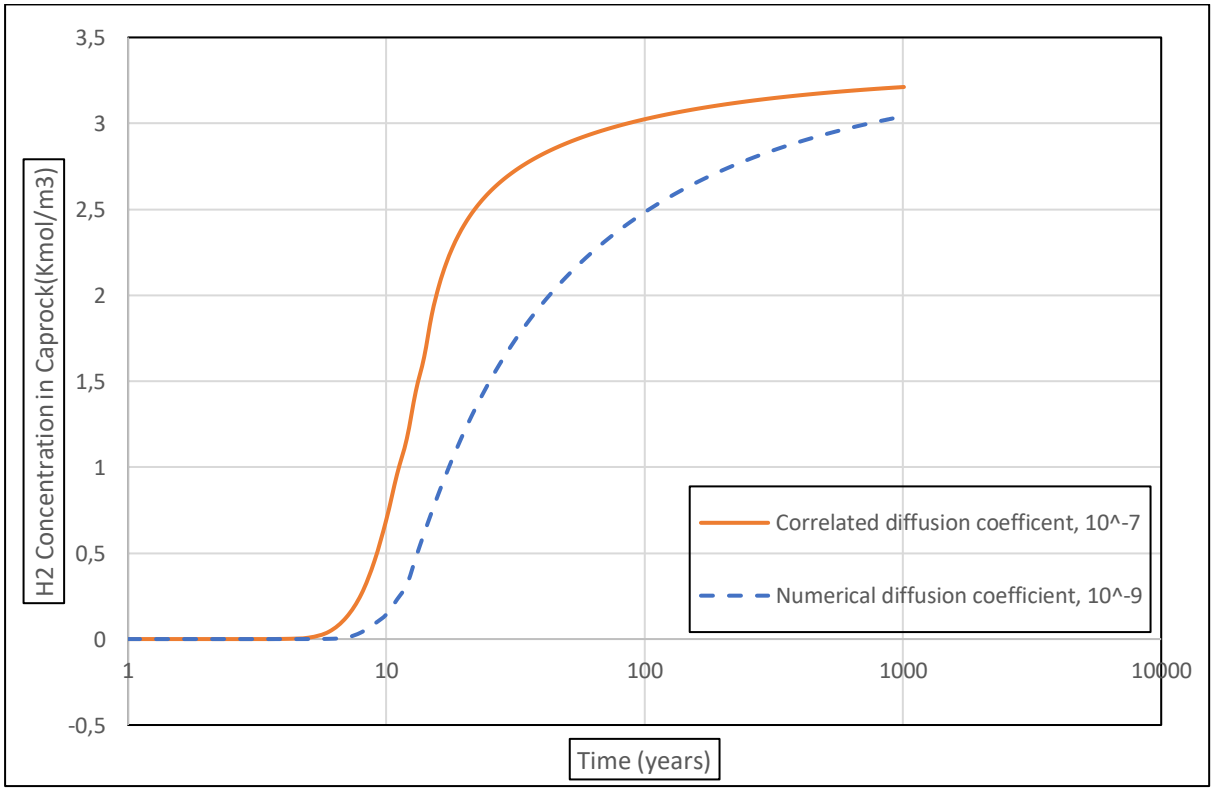


**FIG 4.13:** Diffusion curve for activity corrected diffusion coefficient and diffusion coefficient from correlations.

Based on the results obtained, the correlation calculated diffusion coefficient shows a slow steady increase in concentration in what could be observed as longitudinal progression with respect to time, until a concentration value of 2.5 Kmol/$m^3$ and then further sharp curve increase to a maximum concentration value of 3.3 Kmol/$m^3$ in 1000 years. In another observation for model's diffusion coefficient, the concentration curve increases sharply in time rate to a concentration value of 3.0 Kmol/$m^3$ and at 1000 years. These results further emphasise the need to adopt a recommended diffusion coefficient while simulating the numerical behaviour of gases, especially in diffusion. The reservoir cumulative retention at the model's diffusion coefficient was evaluated at 88 % and that of the correlation gave 83.4 % of the total $H_2$ injected gas. The model's diffusion coefficient $D_i^a$ $10^{-9}m^2/s$ gives a better representation of the diffusivity behaviour of $H_2$ into the caprock.

# Chapter 5: Conclusions and Recommendations

## 5.1 Conclusions

This thesis work provides a comprehensive review and analysis on the diffusion of $H_2$ in the UHS depleted reservoirs. The $H_2$ diffusion was simulated on the effect of HC gas component present in the caprock, variation of temperature, pressure, and porosity of the caprock. The conclusions drawn from the numerical simulations are:

1. On the effects of pressure
    - As pressure varies (from low to high values), its effect on diffusion when a single gas HC component is modelled in the caprock could be seen as increasing the concentration of $H_2$ in the caprock. However, this may vary as HC components go from less dense to denser. At very high pressure and denser HC components (E.g., Pentane), it is observed to inhibit diffusion by giving a low value on concentration. This is because the cross-phased components will move into the pores of the caprock, hence impede on diffusion.
    - As pressure varies (from low to high), its effect on diffusion when a multiple gas HC component is modelled in the caprock could be seen as also increasing the concentration, but this applies visibly to lower binary pairs (E.g., C1+C2). As Pressure increases and decreases temperature, higher HC pairing (E.g., C1+C5), will give a very low concentration profile value and hence diffusion.
2. On the effect of temperature
    - Temperature variation (from lower to higher values) has been shown to also play a role in diffusion of $H_2$. From the results obtained and analysis made, temperature variation when a single component is modelled in the caprock shows that the concentration decreased as temperature is increased. This is explained as when a gas is dissolved in a liquid or present in the pores of a caprock, its solubility and diffusivity are influenced by temperature. With an increase in temperature, the solubility of gases in liquids typically decreases. This is because at higher temperatures, the molecules of the gas and liquid have increased kinetic energy and tend to move more rapidly. This increased molecular motion can disrupt the interactions between gas molecules and liquid

molecules, making it more difficult for the gas to dissolve. Consequently, the concentration of the gas in the liquid or caprock decreases. Although the impact of temperature on binaries could also be observed as giving lower concentration value, it still plays a crucial role in the diffusion process. Therefore, due to the decreased solubility and hindered diffusion caused by increased temperature, the overall diffusion of gases through the caprock in a gas reservoir tends to decrease as temperature increases.

3. On the effect of varying HC components in the caprock
    - The effect of hydrocarbon molecules when they vary from less dense to denser on diffusion, especially as they are dissolved in the pores of the caprock. The dissolved hydrocarbons create a higher chemical potential compared to that of the reservoir that do not contain dissolved hydrocarbons. As a result, the concentration gradient of $H_2$ diffusing through the caprock is affected. The concentration gradient, which is also a factor for this diffusion, affects molecules as they tend to move from regions of higher concentration to regions of lower concentration. However, the presence of dissolved hydrocarbons creates a localized region of higher concentration and higher chemical potential in the caprock. The diffusion of molecules through the caprock is hindered because it would involve moving from regions of lower chemical potential to regions of higher chemical potential (due to the dissolved hydrocarbons). At high pressure and low temperature, the binaries of $C_{1,5}$ has a high effect on diffusion. There seems to be cross-phase, and these yielded less gas saturation values.
4. On the effect of varying porosity
    - It was observed that on varying the porosity same gas concentration was observed as a function of time, but on the cumulative loss, the smaller porosity offered a lower pore volume for diffusion. This shows that less porous caprock is more ideal for UHS operations.

## 5.2 Recommendations

The findings from this thesis work will contribute to the development of safe and efficient storage practices for hydrogen, a critical component of sustainable energy systems. The body

of knowledge can also be applied to the CCSU (Carbon Capture Storage and Utilization) technologies. It also gives a basis for future works in the areas such as:

- Safety Evaluations and risk assessment: the parameters of pressure and temperature can be used to perform thorough safety evaluations pertaining to hydrogen diffusion in UHS systems. Assess the risk of gas accumulating in nearby geological formations and investigate the possibility of hydrogen migration beyond the reservoir boundaries. Create models and procedures for risk assessment to ensure secure storage and avoid unintentional environmental effects.
- Advanced Modeling Methods: To comprehend the molecular-scale mechanisms controlling hydrogen diffusion in UHS systems, using advanced modelling methods such as molecular dynamics simulations, or coupled flow and transport models. These models can shed light on how molecular interactions and diffusion processes affect many aspects of transport behaviour.
- Experimental data validation: it can serve as a solid base to validate the diffusion coefficients and effective diffusion lengths obtained in the current work, through more experimental research. Increase the range of rock porosities, temperature, pressure conditions, and different moisture content levels in the experiment. This will improve the diffusion data's dependability and usefulness in various UHS circumstances.

# References

Amid, A., Mignard, D., & Wilkinson, M. (2016). Seasonal storage of hydrogen in a depleted natural gas reservoir. *International Journal of Hydrogen Energy*, *41*(12), 5549–5558. https://doi.org/10.1016/j.ijhydene.2016.02.036

Ball, M., & Wietschel, M. (2009). The future of hydrogen – opportunities and challenges. *International Journal of Hydrogen Energy*, *34*(2), 615–627. https://doi.org/10.1016/j.ijhydene.2008.11.014

Basu, A., & Singh, R. (1994). *Comparison of Darcy's Law and Fick's Law of Diffusion to Determine the Field Parameters Related to Methane Gas Drainage in Coal Seams*.

B.C Craft, M. H. (2014). *Applied Petroleum Reservoir Engineering. Introduction to Petroleum Reservoirs and Reservoir Engineering*. https://www.informit.com/articles/article.aspx?p=2241145&seqNum=4

Caputo, M., & Plastino, W. (2004). Diffusion in porous layers with memory. *Geophysical Journal International*, *158*(1), 385–396. https://doi.org/10.1111/j.1365-246X.2004.02290.x

Du, F., & Nojabaei, B. (2020). Estimating diffusion coefficients of shale oil, gas, and condensate with nano-confinement effect. *Journal of Petroleum Science and Engineering*, *193*, 107362. https://doi.org/10.1016/j.petrol.2020.107362

Ghaedi, M., Andersen, P. Ø., & Gholami, R. (2023). Hydrogen diffusion into caprock: A semi-analytical solution and a hydrogen loss criterion. *Journal of Energy Storage*, *64*, 107134. https://doi.org/10.1016/j.est.2023.107134

Hassanpouryouzband, A., Adie, K., Cowen, T., Thaysen, E. M., Heinemann, N., Butler, I. B., Wilkinson, M., & Edlmann, K. (2022). Geological Hydrogen Storage: Geochemical

Reactivity of Hydrogen with Sandstone Reservoirs. *ACS Energy Letters*, *7*(7), 2203–2210. https://doi.org/10.1021/acsenergylett.2c01024

Hebei Wansheng Environmental Protection Engineering Co. (2023). *Benefits of Using Anaerobic Digester Tanks*. Hebei Wansheng Environmental Engineering Co., Ltd.

Heinemann, N., Alcalde, J., Miocic, J. M., Hangx, S. J. T., Kallmeyer, J., Ostertag-Henning, C., Hassanpouryouzband, A., Thaysen, E. M., Strobel, G. J., Schmidt-Hattenberger, C., Edlmann, K., Wilkinson, M., Bentham, M., Haszeldine, R. S., Carbonell, R., & Rudloff, A. (2021). Enabling large-scale hydrogen storage in porous media – the scientific challenges. *Energy & Environmental Science*, *14*(2), 853–864. https://doi.org/10.1039/D0EE03536J

Helbæk, M., Hafskjold, B., Dysthe, D. K., & Sørland, G. H. (1996). Self-Diffusion Coefficients of Methane or Ethane Mixtures with Hydrocarbons at High Pressure by NMR. *Journal of Chemical & Engineering Data*, *41*(3), 598–603. https://doi.org/10.1021/je950293p

Hoteit, H. (2011). Proper Modeling of Diffusion in Fractured Reservoirs. *All Days*, SPE-141937-MS. https://doi.org/10.2118/141937-MS

Jafari Raad, S. M., Leonenko, Y., & Hassanzadeh, H. (2022). Hydrogen storage in saline aquifers: Opportunities and challenges. *Renewable and Sustainable Energy Reviews*, *168*, 112846. https://doi.org/10.1016/j.rser.2022.112846

Katarzyna, C. (2020). Insight into a shape of salt storage caverns. *20*. https://yadda.icm.edu.pl/baztech/element/bwmeta1.element.baztech-5fb21964-81ab-4763-bec2-68792069cd7f

Kiran, R., Upadhyay, R., Rajak, V. K., Gupta, S. D., & Pama, H. (2023). Comprehensive study of the underground hydrogen storage potential in the depleted offshore Tapti-gas field. *International Journal of Hydrogen Energy*, *48*(33), 12396–12409. https://doi.org/10.1016/j.ijhydene.2022.12.172

Machado, J. R. S., Streett, W. B., & Dieters, U. (2002, May 1). *PVT measurements of hydrogen/methane mixtures at high pressures* (world). ACS Publications; American Chemical Society. https://doi.org/10.1021/je00052a027

Muhammed, N. S., Haq, M. B., Al Shehri, D. A., Al-Ahmed, A., Rahman, M. M., Zaman, E., & Iglauer, S. (2023). Hydrogen storage in depleted gas reservoirs: A comprehensive review. *Fuel*, *337*, 127032. https://doi.org/10.1016/j.fuel.2022.127032

Oistein, G. (1980). Generalized Pressure-Volume Temperature Correlations. *JOURNAL OF PETROLEUM TECHNOLOGY*.

Ozarslan, A. (2012). Large-scale hydrogen energy storage in salt caverns. *International Journal of Hydrogen Energy*, *37*(19), 14265–14277. https://doi.org/10.1016/j.ijhydene.2012.07.111

Reitenbach, V., Ganzer, L., Albrecht, D., & Hagemann, B. (2015). Influence of added hydrogen on underground gas storage: A review of key issues. *Environmental Earth Sciences*, *73*(11), 6927–6937. https://doi.org/10.1007/s12665-015-4176-2

Riazi, M. R. (1996). A new method for experimental measurement of diffusion coefficients in reservoir fluids. *Journal of Petroleum Science and Engineering*, *14*(3), 235–250. https://doi.org/10.1016/0920-4105(95)00035-6

Shafikova, G. M. (2013). *Analysis of Diffusion Models in Eclipse 300*. https://ntnuopen.ntnu.no/ntnu-xmlui/handle/11250/240233

Sigmund, P. M. (1976). Prediction of Molecular Diffusion at Reservoir Conditions. Part II - Estimating the Effects of Molecular Diffusion and Convective Mixing in Multicomponent Systems. *Journal of Canadian Petroleum Technology*, *15*(03). https://doi.org/10.2118/76-03-07

Storey, S. (2013). Natural Gas Storage Basics. *Sever | Storey*. https://landownerattorneys.com/natural-gas-storage-basics/

Tarkowski, R. (2019). Underground hydrogen storage: Characteristics and prospects. *Renewable and Sustainable Energy Reviews*, *105*, 86–94. https://doi.org/10.1016/j.rser.2019.01.051

Widyanita, A., Cai, J. Z., Mat, M., Ali, S., Hamid, M., & Jones, E. (2021, March 16). *Gas Migration Mechanisms and Their Effects on Caprock Seal Capacity: A Case Study in Depleted Gas Fields in the Sarawak Basin, Offshore Malaysia*. https://doi.org/10.2523/IPTC-21494-MS

Xue, Y., Liu, J., Dang, F., Liang, X., Wang, S., & Ma, Z. (2020). Influence of CH4 adsorption diffusion and CH4-water two-phase flow on sealing efficiency of caprock in underground energy storage. *Sustainable Energy Technologies and Assessments*, *42*, 100874. https://doi.org/10.1016/j.seta.2020.100874

# Declaration of non-conflict of interests

I, Darlington Ekene Ekemezie, hereby affirm that I have no conflicts of interest that might compromise the objectivity, or impartiality of my study or its findings about the completion of my thesis work. This also applies to all financial, professional, and academic relationships that may have an impact on the ideas or conclusions in my thesis.

*Darlington Ekenedilichukwu Ekemezie,*

*UiS 2023.*